Application of Machine Learning in Hadron Physics

Qian Wang (王倩)
qianwang@m.scnu.edu.cn

第八届强子谱和强子结构研讨会
桂林 广西师范大学 2025年7月11日-15日

AI 百年发展

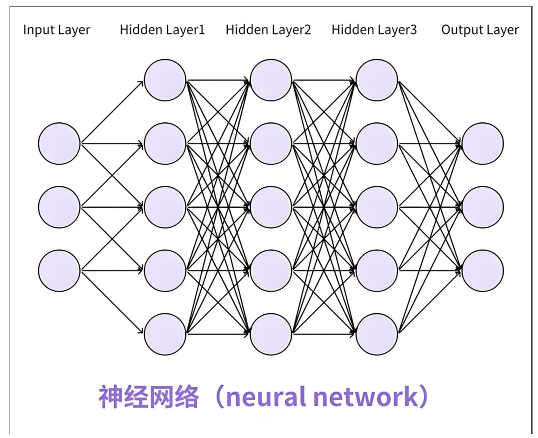

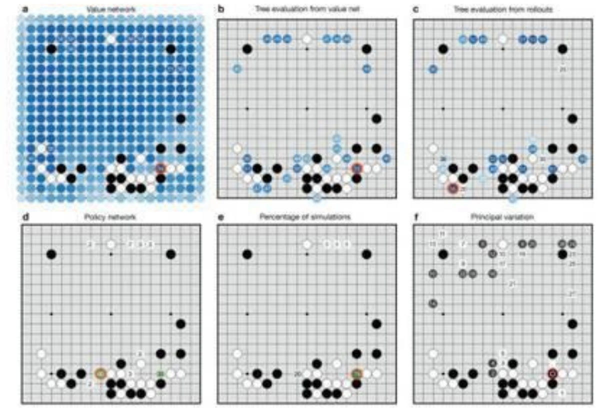

AlphaGo

科学大模型？

2022

CHAT GPT

2018

AlphaGo
围棋

人工智能大模型
ChatGPT 问世

1980-1987
“专家系统”

2016

AlphaFold
蛋白质结构预测

1941-1974
早期人工智能

2005-今
飞速发展

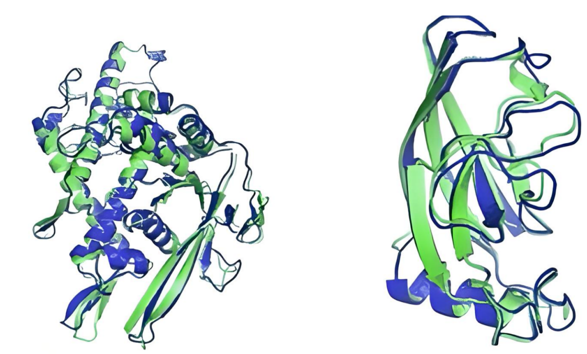

T1037 / 6vr4
90.7 GDT
(RNA polymerase domain)

T1049 / 6y4f
93.3 GDT
(adhesin tip)

AI 技术飞速发展，正在掀起一场新的科技革命

参考 段文辉 院士 2025年 彭桓武讲座 报告

Machine learning in physics

- Quantum many-body problem

- Quantum states based on artificial neural networks

⇒ Use neural network to learn many-body wave function

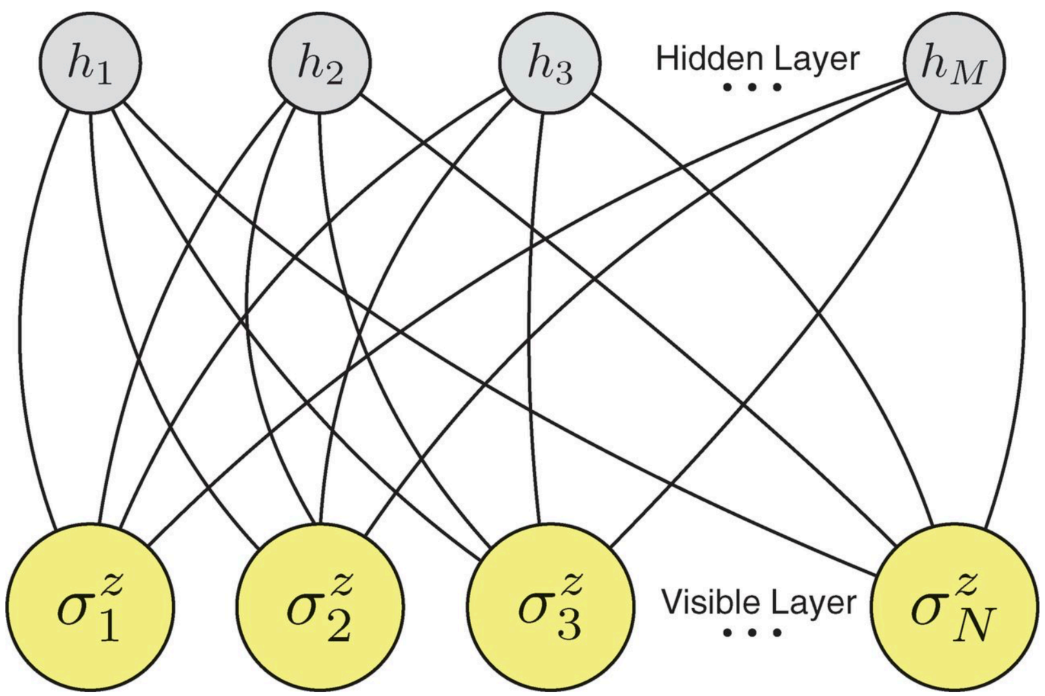

Carleo, Torcer, Science 355(2017)602-606

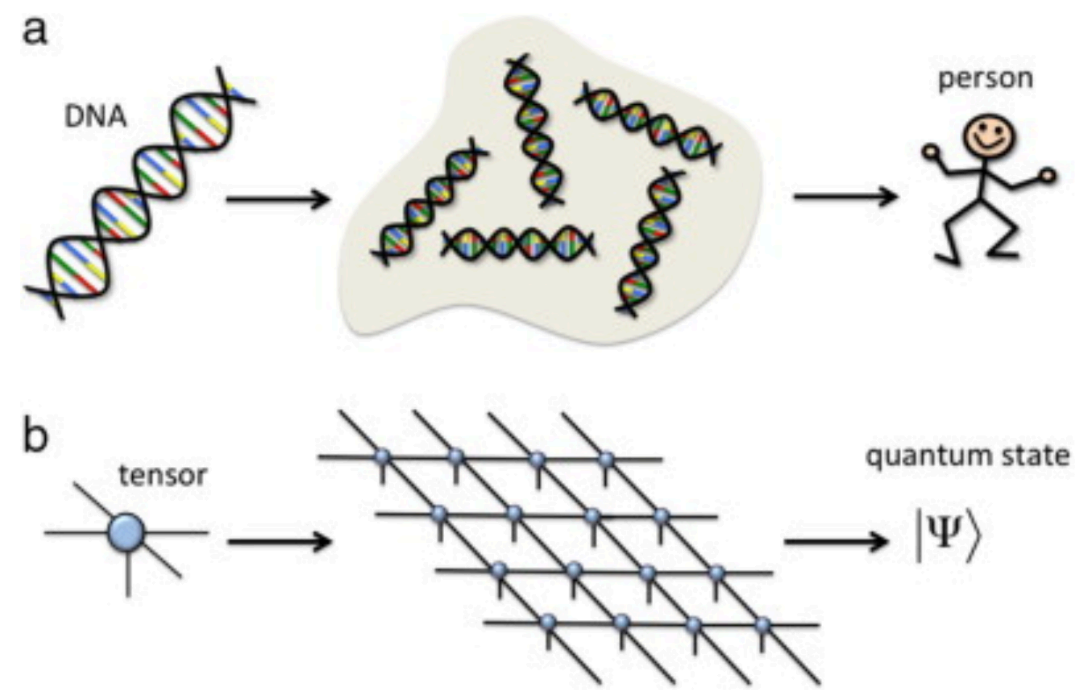

- Tensor network and Automatic differentiation

⇒ Solve high-dimensional strong correlation problems

Orus, Annals Phys.349(2014)117-158

Machine learning in physics

- Particle physics and cosmology

- Data analysis

Baldi et al., Nat. Commun. 5 (2014) 4308

⇒ Particle trajectory and jet classification

Alexandru et al., PRD96(2017)094505,

Kanwar et al., PRL125(2020)121601

- Accelerate LQCD simulation

⇒ Manifold sampling solves sign problem and generate samples

Shi et al., PRD105(2022)014017

- Solve inverse problem

⇒ Physical states during hadronization

- Cosmology

⇒ Detect small-scale structures in the early universe

Sun et al., arXiv:2407.14298

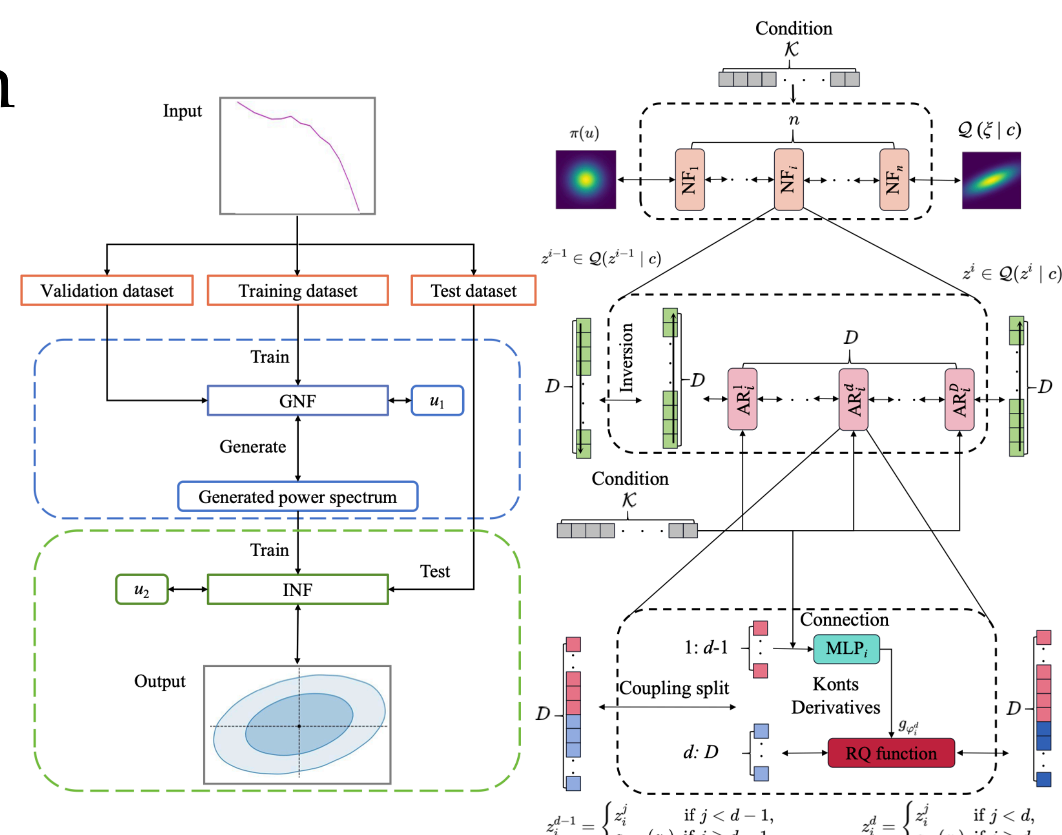

Machine learning in physics

- Physics-driven machine learning

- Discover physical laws

Schmidt and Lipson, Science 324(2009)81-85

⇒ Conservation and symmetries

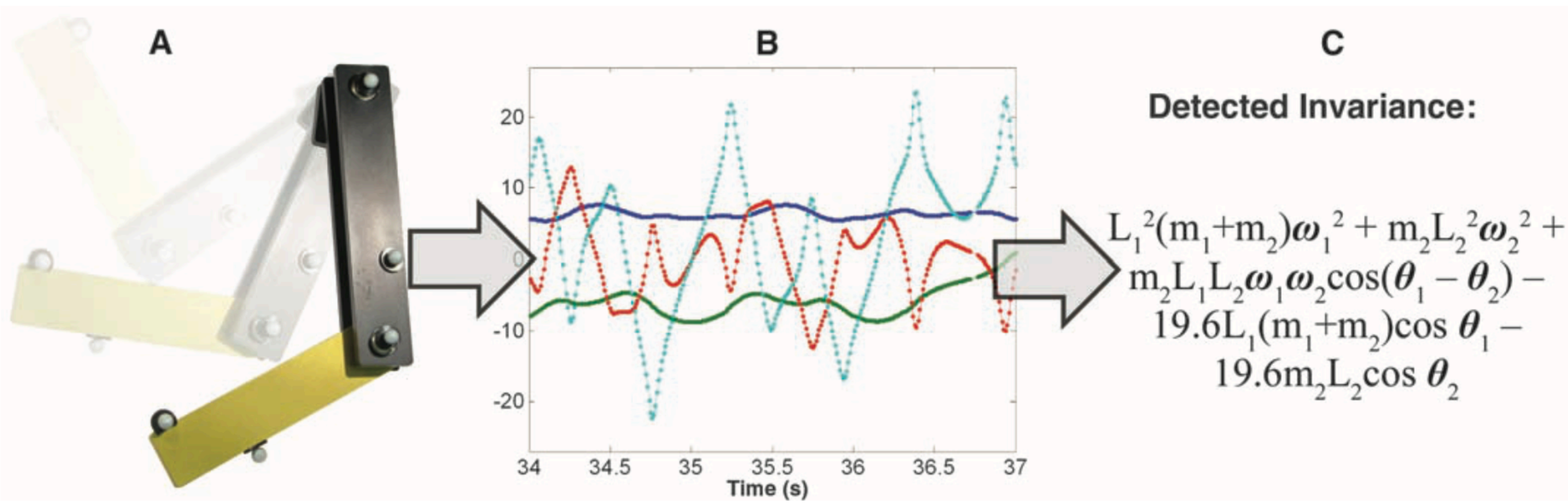

- Physics-informed neural networks

Raissi et al, J. Compute. Phys. 378(2019)686-707

⇒ Solve problems related to partial differential equations

Machine learning in physics

- Heavy ion physics

- Interpretable ML in jet background subtraction in HIC

  Mengel et al., PRC108(2023)L021901

- An equation of state meter of quantum chromodynamics transition from deep learning

  Pang et al., Nat. Commun. 9(2018)210

- Jet tomography in HIC with deep learning

  Du et al., PRL128(2022)012301

- ML-based jet momentum reconstruction in HIC

  Haake et al., PRC99(2019)064904

- Deep Learning for the classification of quenched jets

  Apolinario et al., JHEP11(2021)219

- Probing HIC using quark and gluon jet substructure with ML

  Chien, NPA982(2019)619-622

- ……

Machine learning in hadron physics

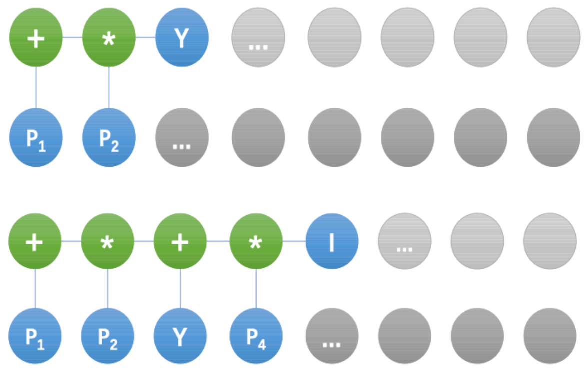

Regress Gell-Mann-Okubo formula

CPL39(2022)111201

2022

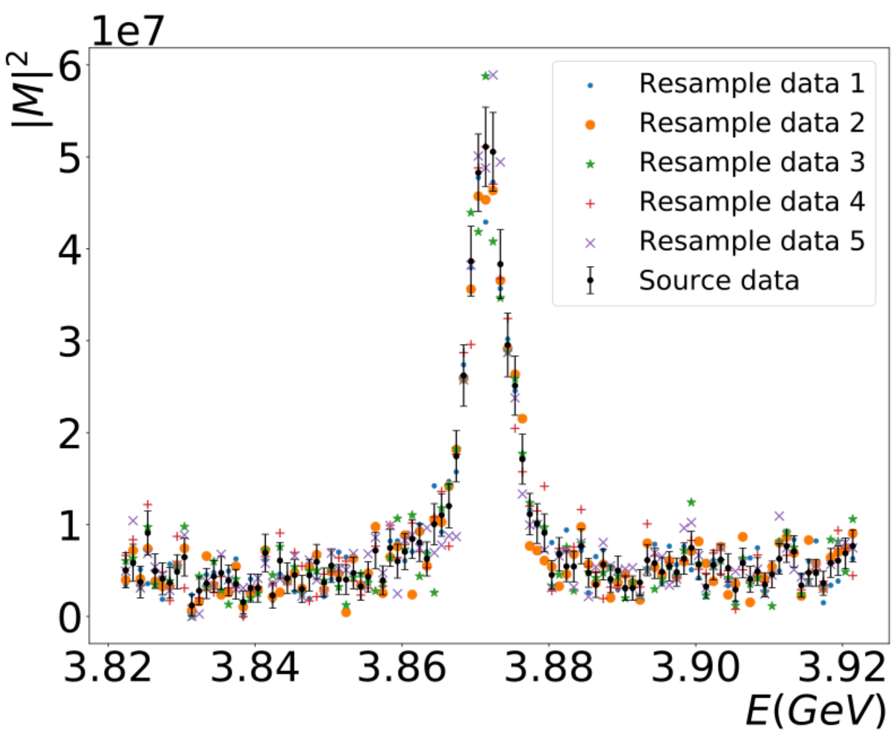

One-channel analysis

PRD105(2022)076013

Machine learning in hadron physics

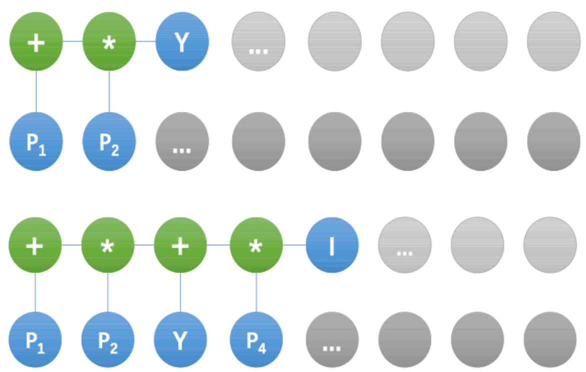

Regress Gell-Mann-Okubo formula

CPL39(2022)111201

2022

2023

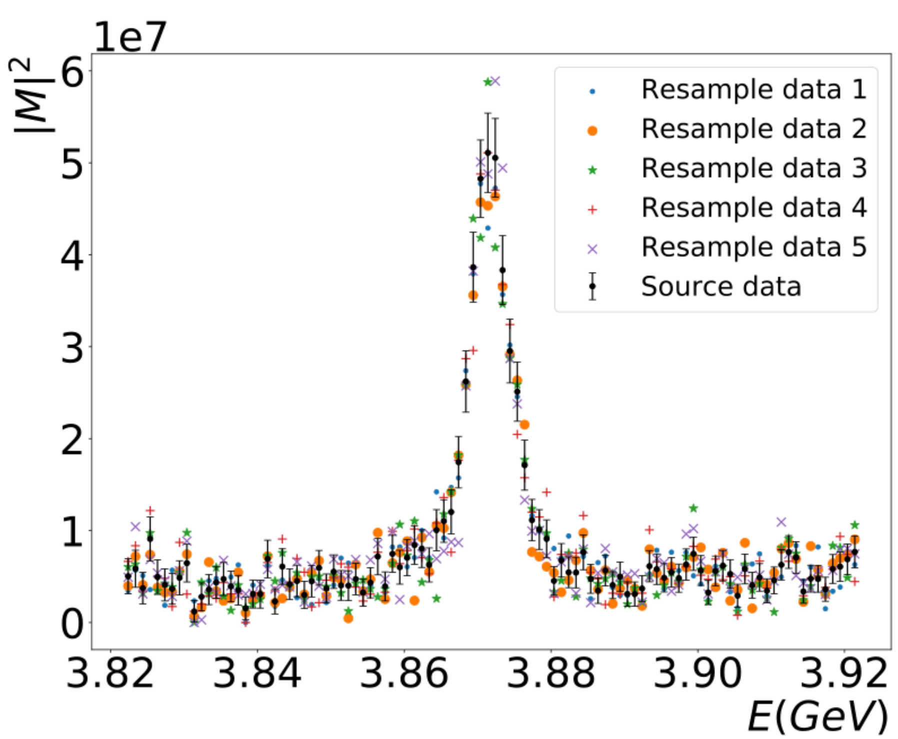

One-channel analysis

PRD105(2022)076013

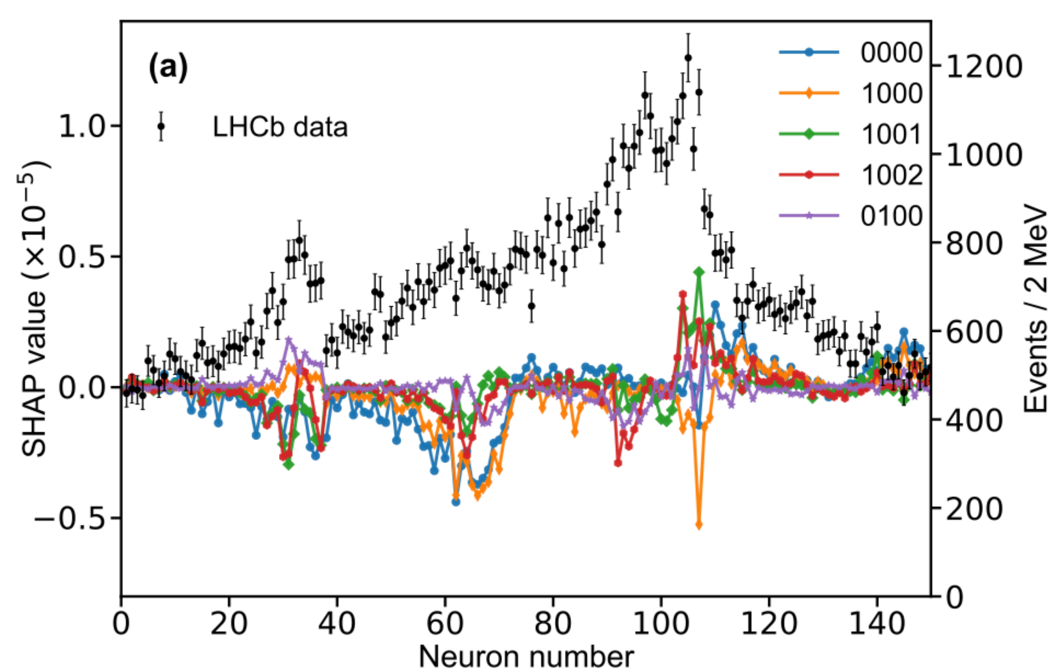

Coupled channel analysis

Sci.Bull.68(2023)981

Machine learning in hadron physics

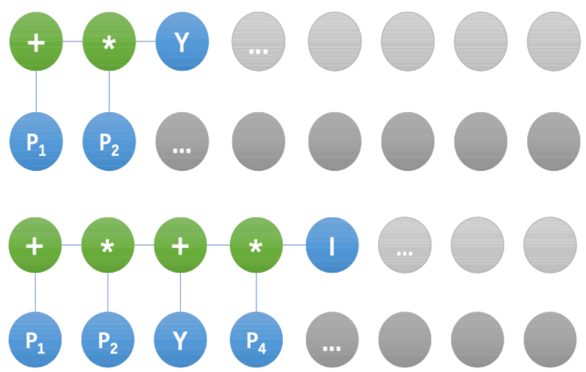

Regress Gell-Mann-Okubo formula

CPL39(2022)111201

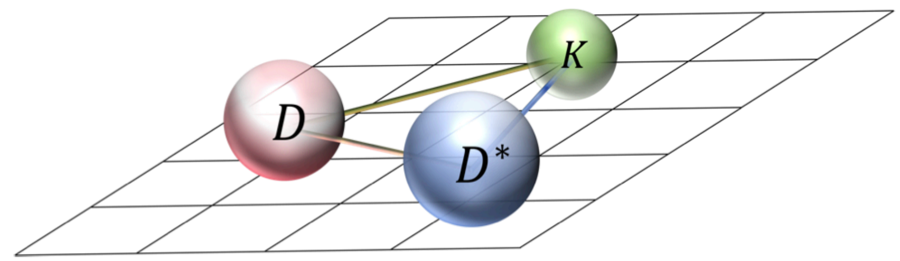

Three-body system on the lattice

PRD(2025)036002

2022

2023

2024

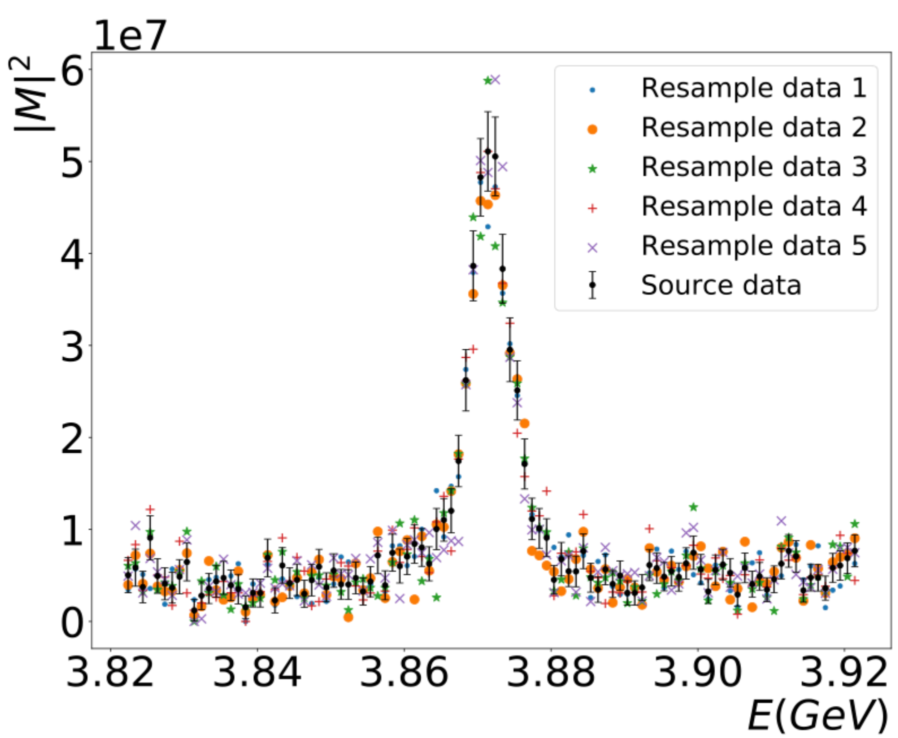

One-channel analysis

PRD105(2022)076013

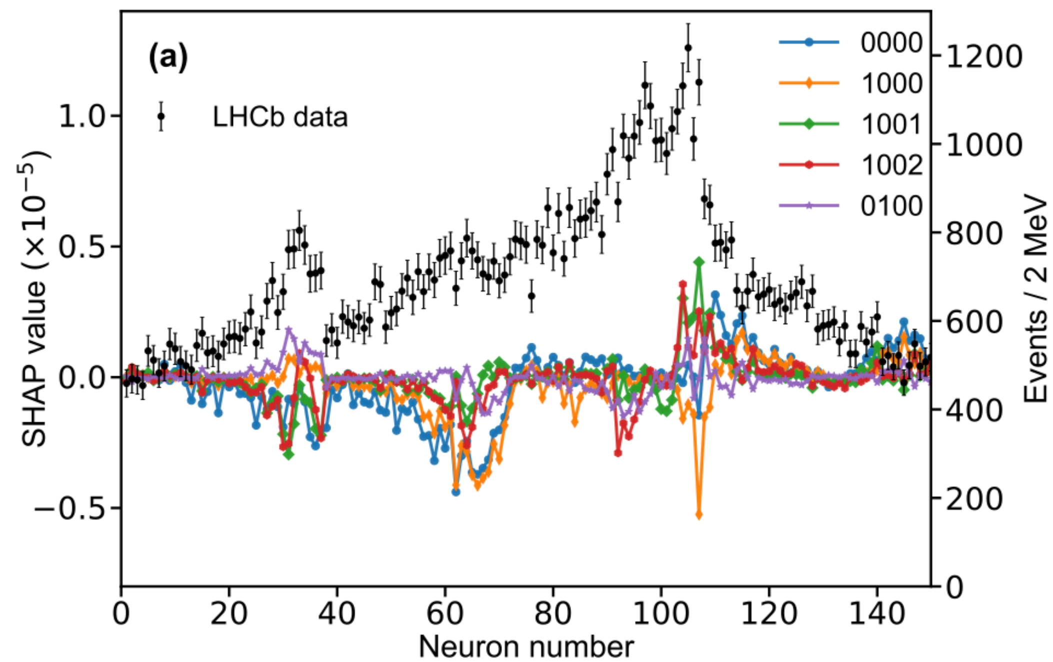

Coupled channel analysis

Sci.Bull.68(2023)981

Machine learning in hadron physics

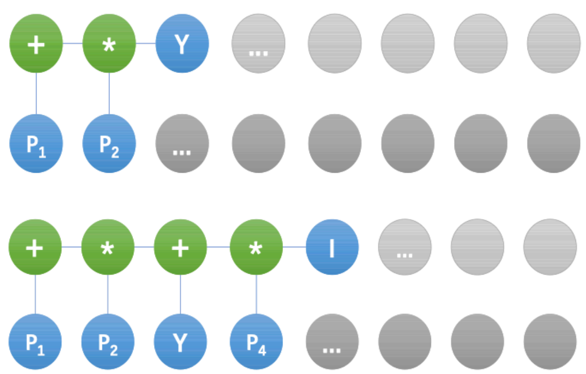

Regress Gell-Mann-Okubo formula

CPL39(2022)111201

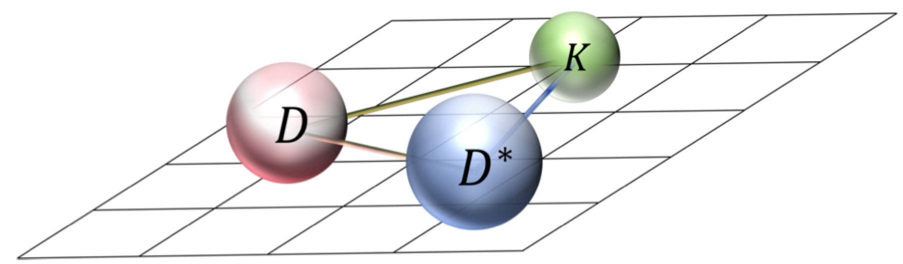

Three-body system on the lattice

PRD(2025)036002

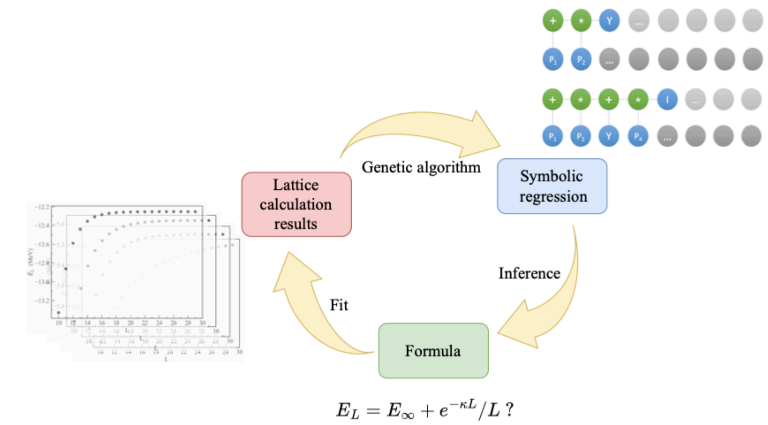

The power law of FV energy shift

arXiv:2503.06496

2022 — 2023 — 2024 — 2025

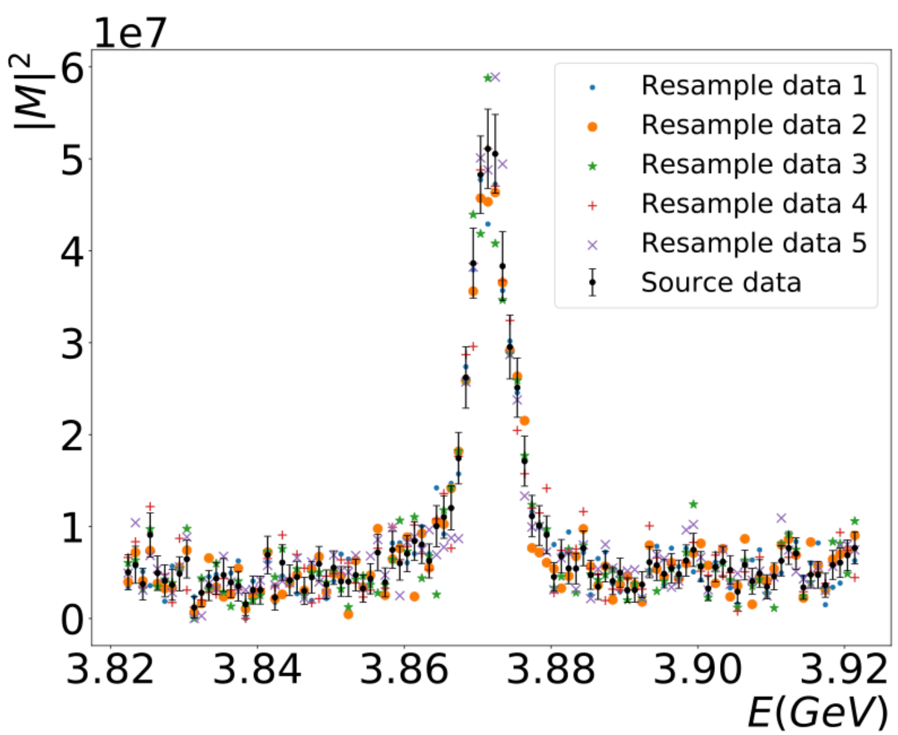

One-channel analysis

PRD105(2022)076013

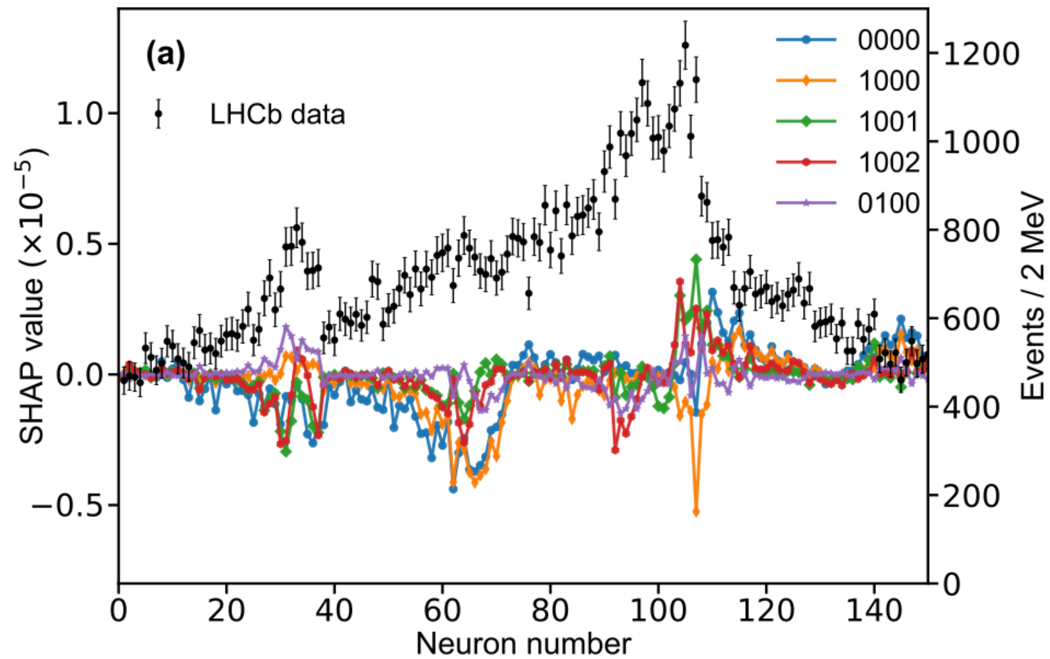

Coupled channel analysis

Sci.Bull.68(2023)981

Workflow

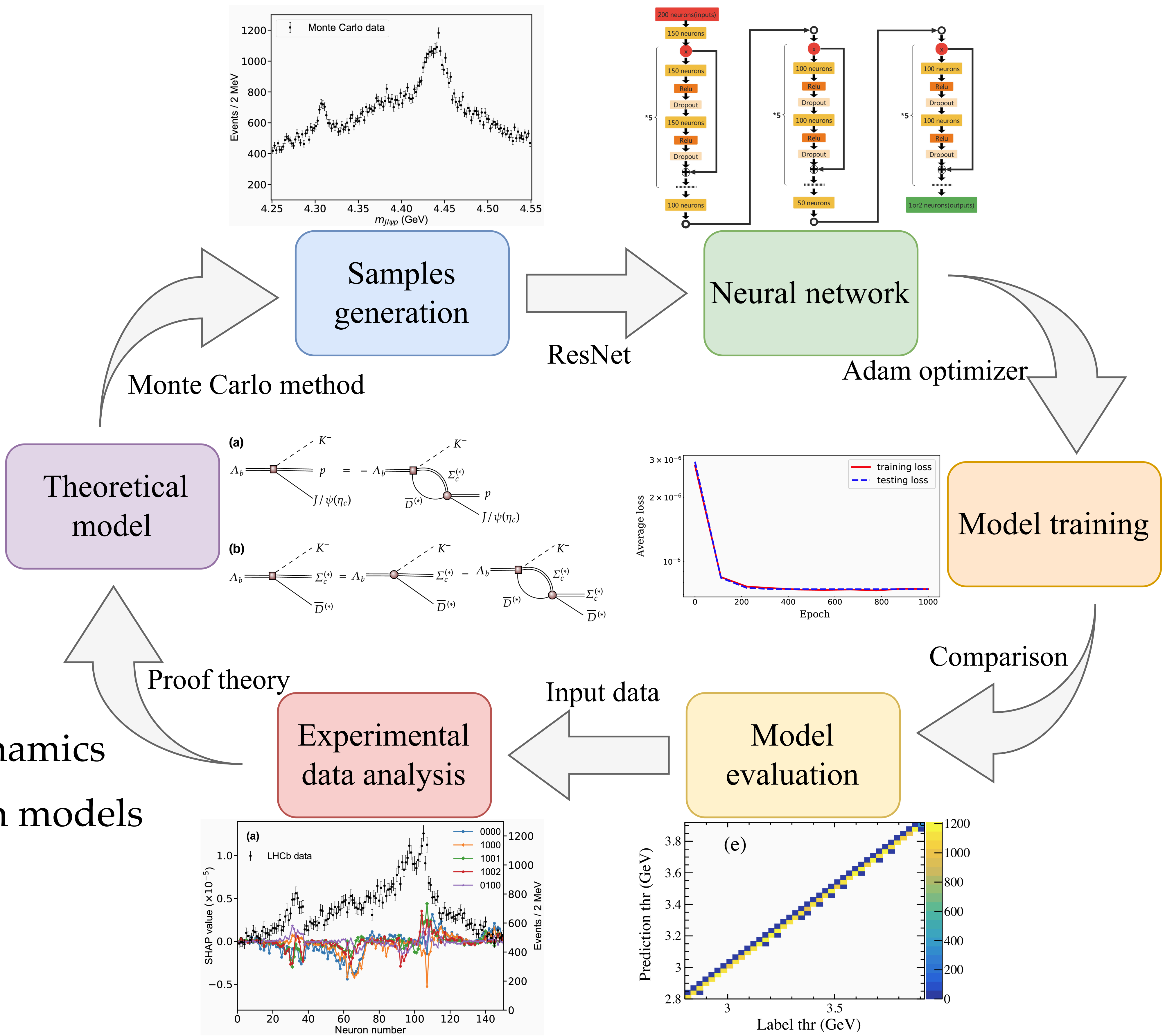

Extract dynamics

Distinguish models

One-channel case in 2022

The first step: One-channel line shape in HM picture

Why one-channel case?

- The most simple case
- A given structure has one foremost channel
- In the isospin limit, sometimes the requirement can be satisfied

$X(3872) \quad D\bar{D}^* + c.c.$

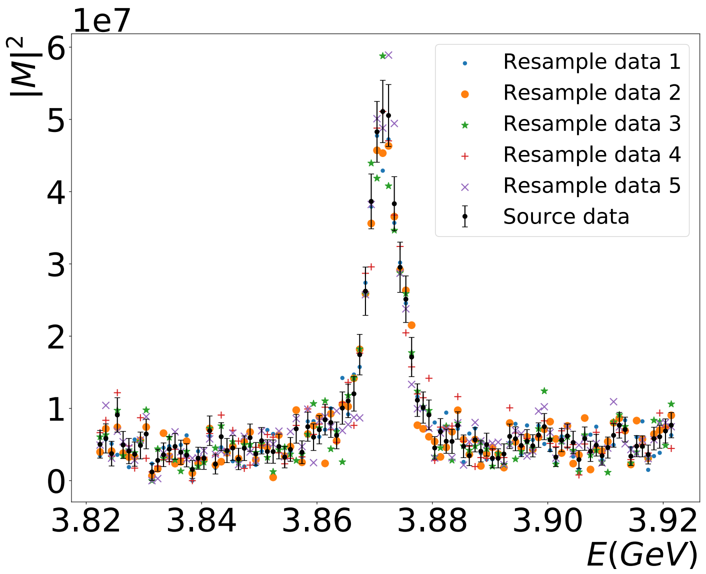

$T_{cc}^{+} \quad DD^*$

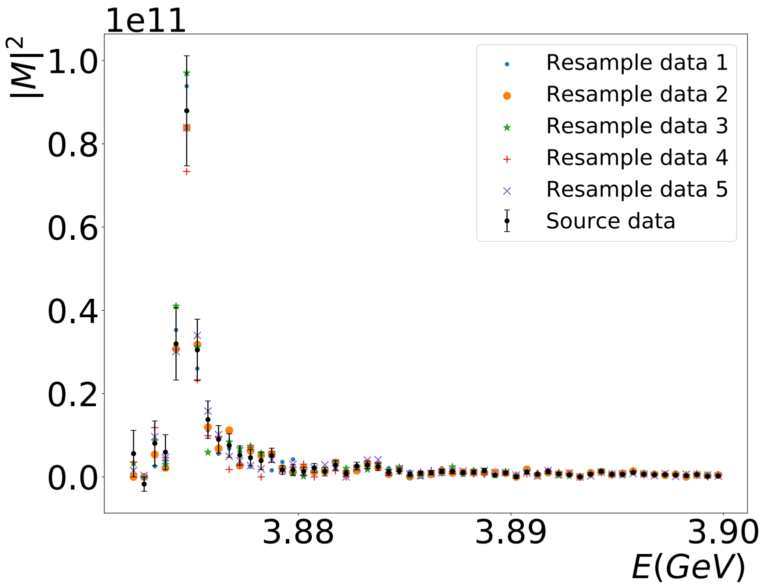

Liu, Zhang, Hu, **QW**, PRD105(2022)076013

One-channel case in 2022

Generate samples

Choose parameter region

$$
\begin{aligned}
a &\in [4.93, 14.80] \ \text{fm}, \\
r &\in [0.49, 0.99] \cup [-9.87, -0.49] \ \text{fm}, \\
m_1 + m_2 &\in [2.8, 3.9] \ \text{GeV}, \\
\sigma &\in [0.5, 10] \ \text{MeV}.
\end{aligned}
$$

- Allow for bound state, virtual state and resonances
- Cover charmonium(-like) region
- Resolution is set to cover usual experimental values
- Generate 150000 samples (100 data points)
- 45000 samples for testing

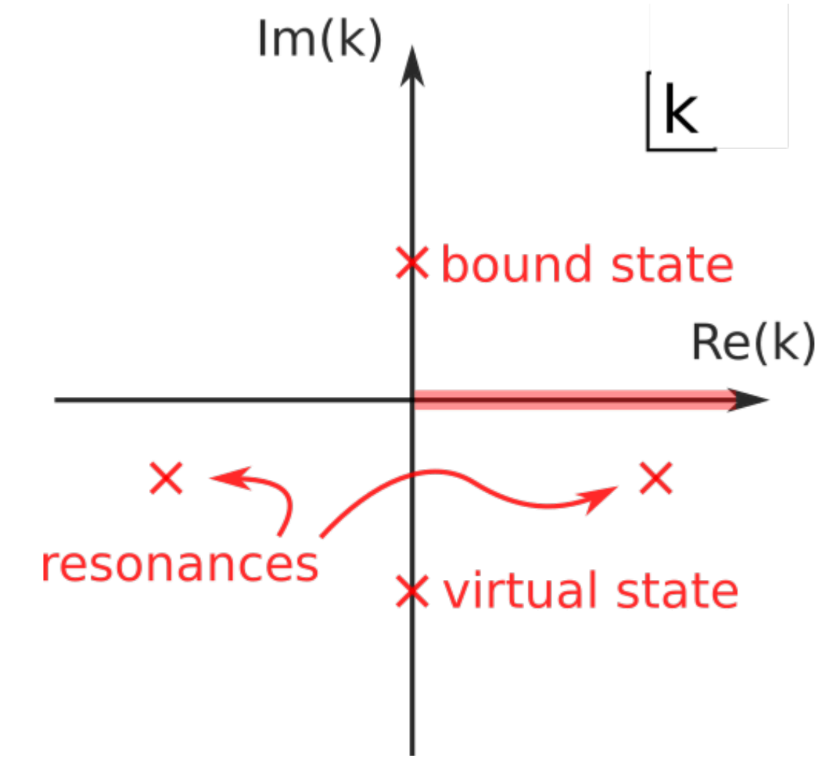

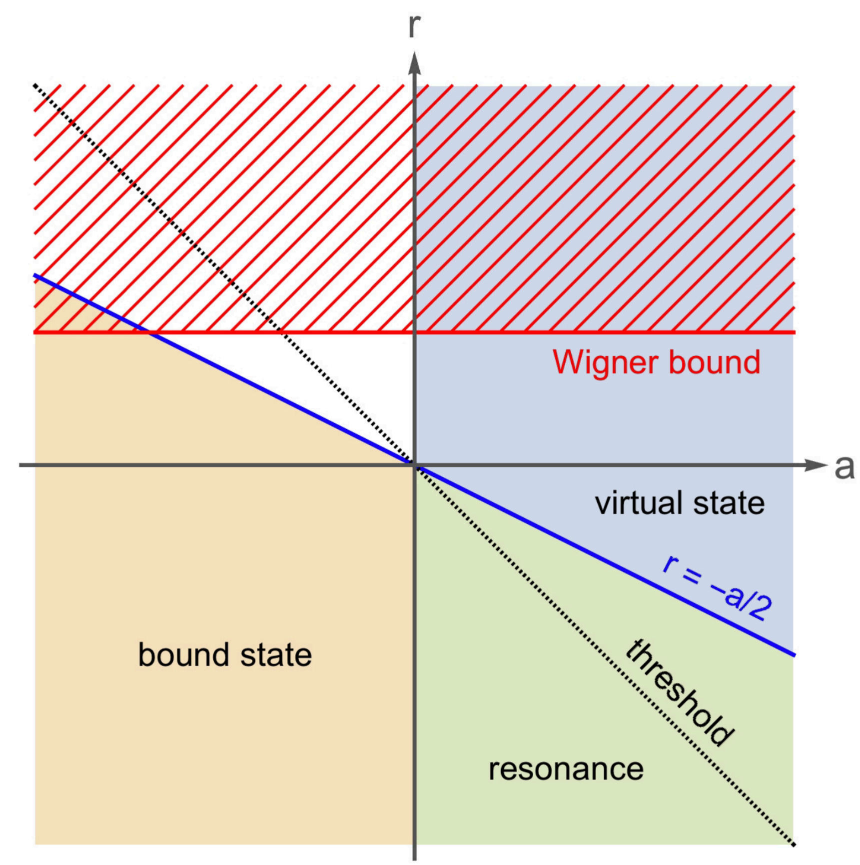

Matuschek, **Baru, Guo, Hanhart**, EPJA57(2021)101

One-channel case in 2022

Evaluation

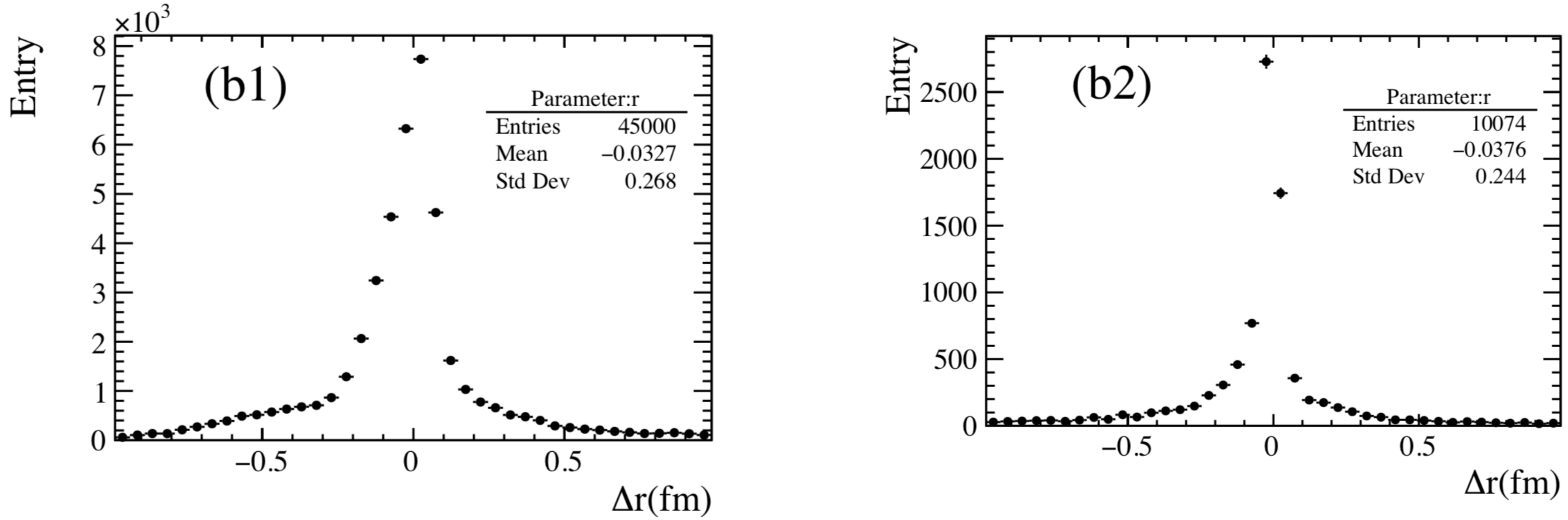

- The difference between the predicted values and the label values.
- The distributions are obtained by testing 45000 samples.
- The means measure the deviation of the predicted values from the label ones.
- The root-of-mean-square (RMS) measures the intrinsic uncertainties.
- Compare to the 10074/45000 fitting results.

Liu, Zhang, Hu, **QW**, PRD105(2022)076013

One-channel case in 2022

Evaluation

Liu, Zhang, Hu, **QW**, PRD105(2022)076013

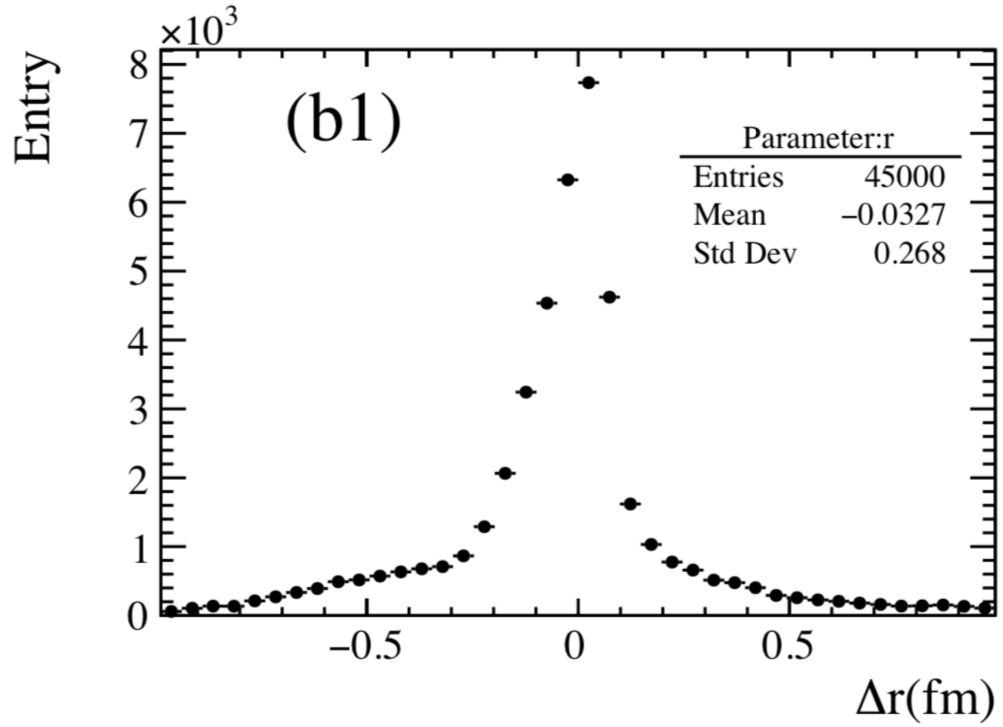

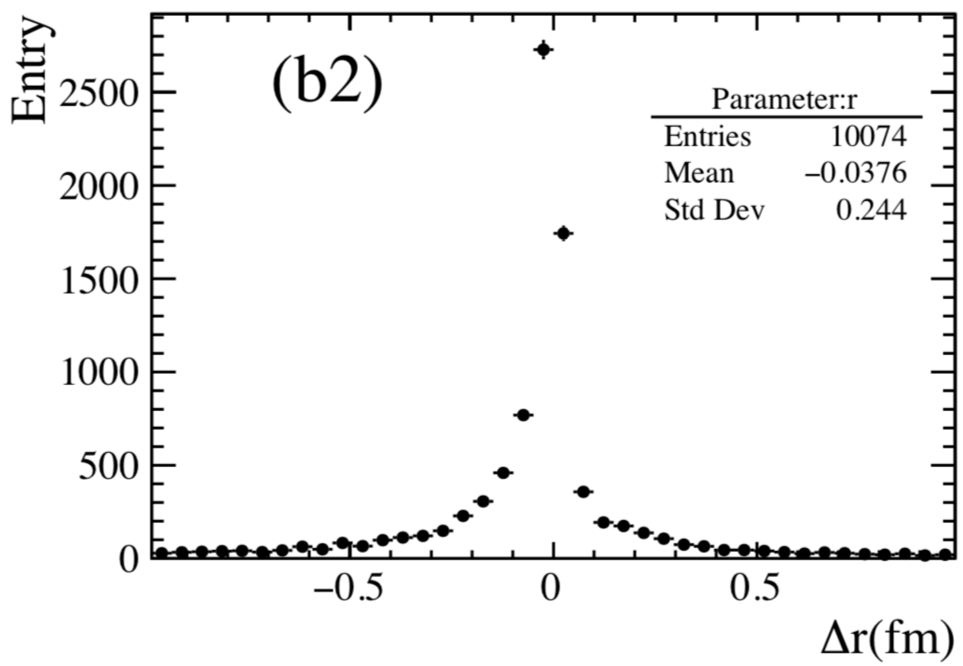

Table I. The biases and errors information of models

methods→	Deep learning		Fitting	
parameters↓	bias	uncertainty	bias	uncertainty
a (fm)	-0.010	1.040	-1.67	2.740
r (fm)	-0.033	0.268	-0.038	0.244
threshold (MeV)	0.75	0.52	-0.16	0.31
σ (MeV)	-0.0001	0.06	-0.0098	0.10

One-channel case in 2022

Apply to the $X(3872)$

Liu, Zhang, Hu, **QW**, PRD105(2022)076013

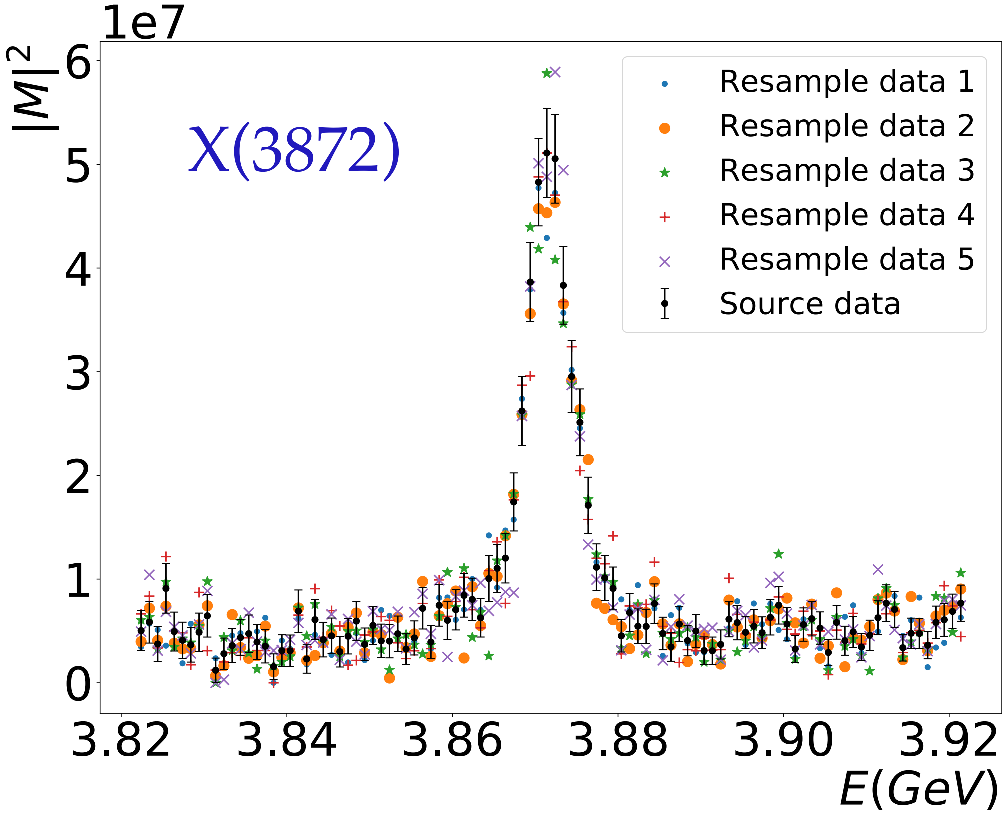

- $D\bar{D}^* + c.c.$ channel
- a, r and threshold are consistent with those from fitting within 1σ
- The errors are obtained in bootstrap (10000 data sets)

$\boldsymbol{X(3872)}$ **parameters**	Deep Learning	Fit
parameter a (fm)	8.76 ± 1.75	9.95 ± 0.34
parameter r (fm)	0.56 ± 0.55	0.32 ± 0.08
parameter threshold (MeV)	3871.30 ± 0.52	3871.20 ± 0.01
parameter σ (MeV)	1.20 ± 0.15	1.70 ± 0.16

One-channel case in 2022

Apply to the T_{cc}^{+}

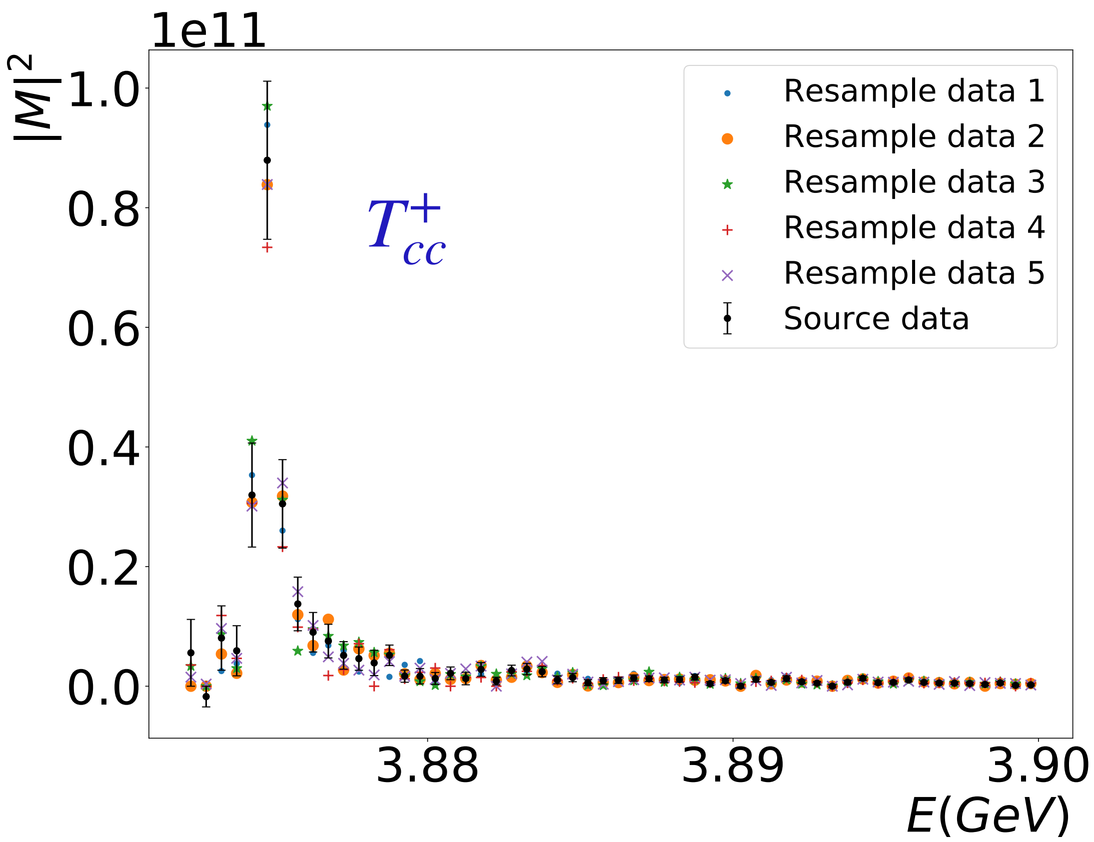

- DD^* channel
- a, r and threshold are consistent with those from fitting within 1σ
- The errors are obtained in bootstrap (10000 data sets)

T_{cc}^{+} **parameters**	Deep Learning	Fit
parameter a (fm)	8.23 ± 1.04	13.74 ± 4.77
parameter r (fm)	-2.79 ± 0.27	-2.15 ± 0.21
parameter threshold (MeV)	3874.83 ± 0.51	3874.53 ± 0.13
parameter σ (MeV)	1.10 ± 0.06	0.11 ± 0.12

Liu, Zhang, Hu, **QW**, PRD105(2022)076013

One-channel case in 2022

Apply to the T_{cc}^+

ML can do as good as normal fitting approach

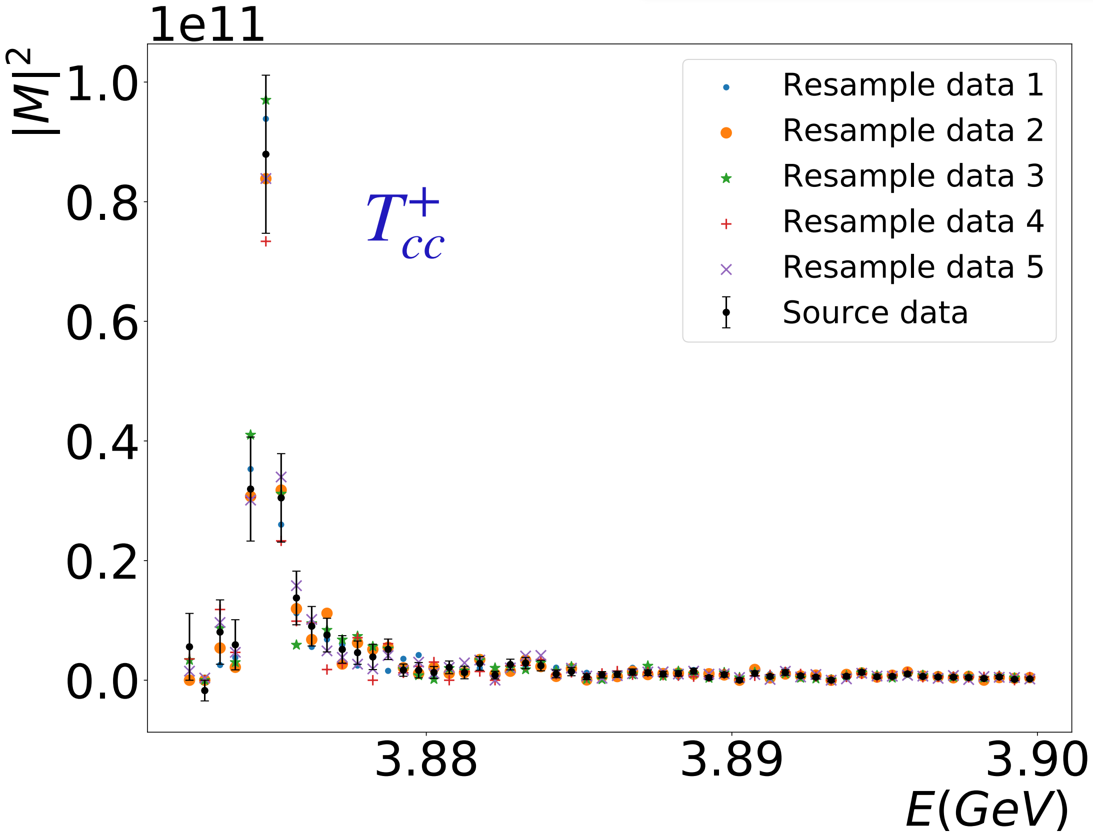

- DD^* channel
- a, r and threshold are consistent with those from fitting within 1σ
- The errors are obtained in bootstrap (10000 data sets)

T_{cc}^+ **parameters**	Deep Learning	Fit
parameter a (fm)	8.23 ± 1.04	13.74 ± 4.77
parameter r (fm)	-2.79 ± 0.27	-2.15 ± 0.21
parameter threshold (MeV)	3874.83 ± 0.51	3874.53 ± 0.13
parameter σ (MeV)	1.10 ± 0.06	0.11 ± 0.12

Liu, Zhang, Hu, **QW**, PRD105(2022)076013

Multi-channel case in 2023

The history of pentaquarks **Bing-Song Zou**, Sci.Bull.66(2021)1258

$\Lambda(1405)$ predicted by Dalitz and Tuan in 1959 Dalitz and Tuan, PRL2(1959)425

- An excited state of a three-quark (uds) system
- $\bar{K}N$ hadronic molecule with $udsq\bar{q}$

A similar situation for $N^\star(1535)$

- An excited state of a three-quark (uds) system
- $\bar{K}\Sigma - \bar{K}\Lambda$ dynamical generated state with $qqqs\bar{s}$ **Kaiser**, Siegel, **Weise**, NPA594(1995)325

Pentaquark in hidden charm sector

Liu, **Zou**, PRL96(2006)042002

Wu, Molina, Oset, **Zou**, PRL105(2010)232001

(I,S)	z_R (MeV)	g_a		
$(1/2,0)$		$\bar{D}\Sigma_c$	$\bar{D}\Lambda_c^+$	
	4269	2.85	0	
$(0,-1)$		$\bar{D}_s\Lambda_c^+$	$\bar{D}\Xi_c$	$\bar{D}\Xi_c'$
	4213	1.37	3.25	0
	4403	0	0	2.64

(I,S)	z_R (MeV)	g_a		
$(1/2,0)$		$\bar{D}^*\Sigma_c$	$\bar{D}^*\Lambda_c^+$	
	4418	2.75	0	
$(0,-1)$		$\bar{D}^*_s\Lambda_c^+$	$\bar{D}^*\Xi_c$	$\bar{D}^*\Xi_c'$
	4370	1.23	3.14	0
	4550	0	0	2.53

Multi-channel case in 2023

The $\Sigma_c^{(*)}\bar{D}^{(*)}$ molecular picture

Liu et.al., PRL122(2019)242001

Scenario	Molecule	J^P	B (MeV)	M (MeV)
A	$\bar{D}\Sigma_c$	$\frac{1}{2}^-$	7.8 – 9.0	4311.8 – 4313.0
A	$\bar{D}\Sigma_c^*$	$\frac{3}{2}^-$	8.3 – 9.2	4376.1 – 4377.0
A	$\bar{D}^*\Sigma_c$	$\frac{1}{2}^-$	Input	4440.3
A	$\bar{D}^*\Sigma_c$	$\frac{3}{2}^-$	Input	4457.3
A	$\bar{D}^*\Sigma_c^*$	$\frac{1}{2}^-$	25.7 – 26.5	4500.2 – 4501.0
A	$\bar{D}^*\Sigma_c^*$	$\frac{3}{2}^-$	15.9 – 16.1	4510.6 – 4510.8
A	$\bar{D}^*\Sigma_c^*$	$\frac{5}{2}^-$	3.2 – 3.5	4523.3 – 4523.6
B	$\bar{D}\Sigma_c$	$\frac{1}{2}^-$	13.1 – 14.5	4306.3 – 4307.7
B	$\bar{D}\Sigma_c^*$	$\frac{3}{2}^-$	13.6 – 14.8	4370.5 – 4371.7
B	$\bar{D}^*\Sigma_c$	$\frac{1}{2}^-$	Input	4457.3
B	$\bar{D}^*\Sigma_c$	$\frac{3}{2}^-$	Input	4440.3
B	$\bar{D}^*\Sigma_c^*$	$\frac{1}{2}^-$	3.1 – 3.5	4523.2 – 4523.6
B	$\bar{D}^*\Sigma_c^*$	$\frac{3}{2}^-$	10.1 – 10.2	4516.5 – 4516.6
B	$\bar{D}^*\Sigma_c^*$	$\frac{5}{2}^-$	25.7 – 26.5	4500.2 – 4501.0

- Two parameters determined by

$P_c(4440),\ P_c(4457)$

- Two solutions

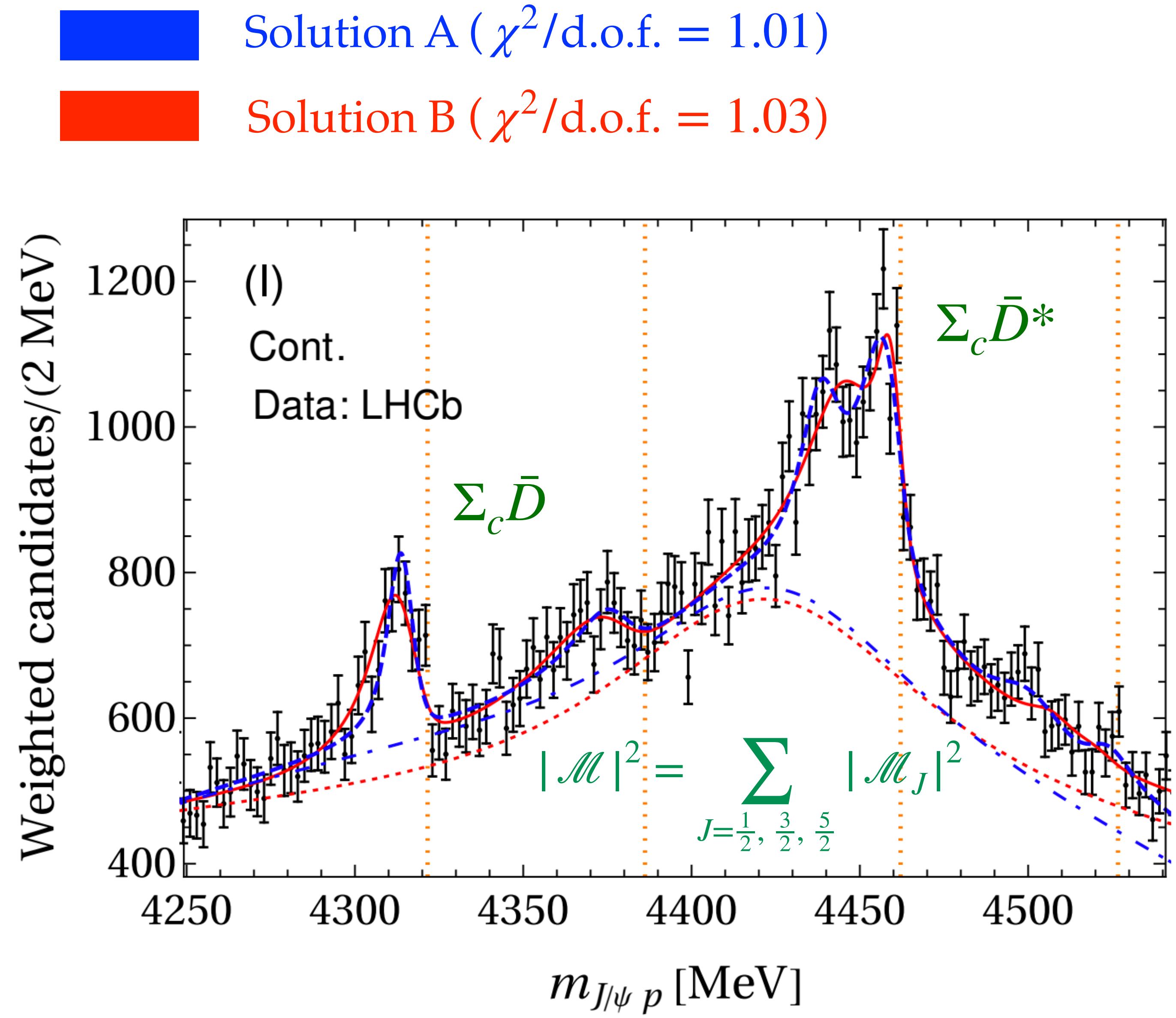

- Two parameters $g_S,\ g_D$ for $J/\psi p,\ \eta_c p$
- Predict pole positions accurately
- $\chi^2_A < \chi^2_B$
- The effect of each data point is different

Du, Baru, Guo, Hanhart, Meißner, Oller, **QW,** PRL124(2020)072001

Multi-channel case in 2023

The $\Sigma_c^{(*)}\bar{D}^{(*)}$ molecular picture

Liu et.al., PRL122(2019)242001

Solution A ($\chi^2/\text{d.o.f.} = 1.01$)

Solution B ($\chi^2/\text{d.o.f.} = 1.03$)

Scenario	Molecule	J^P	B (MeV)	M (MeV)
A	$\bar{D}\Sigma_c$	$\frac{1}{2}^-$	7.8 – 9.0	4311.8 – 4313.0
A	$\bar{D}\Sigma_c^*$	$\frac{3}{2}^-$	8.3 – 9.2	4376.1 – 4377.0
A	$\bar{D}^*\Sigma_c$	$\frac{1}{2}^-$	Input	4440.3
A	$\bar{D}^*\Sigma_c$	$\frac{3}{2}^-$	Input	4457.3
A	$\bar{D}^*\Sigma_c^*$	$\frac{1}{2}^-$	25.7 – 26.5	4500.2 – 4501.0
A	$\bar{D}^*\Sigma_c^*$	$\frac{3}{2}^-$	15.9 – 16.1	4510.6 – 4510.8
A	$\bar{D}^*\Sigma_c^*$	$\frac{5}{2}^-$	3.2 – 3.5	4523.3 – 4523.6
B	$\bar{D}\Sigma_c$	$\frac{1}{2}^-$	13.1 – 14.5	4306.3 – 4307.7
B	$\bar{D}\Sigma_c^*$	$\frac{3}{2}^-$	13.6 – 14.8	4370.5 – 4371.7
B	$\bar{D}^*\Sigma_c$	$\frac{1}{2}^-$	Input	4457.3
B	$\bar{D}^*\Sigma_c$	$\frac{3}{2}^-$	Input	4440.3
B	$\bar{D}^*\Sigma_c^*$	$\frac{1}{2}^-$	3.1 – 3.5	4523.2 – 4523.6
B	$\bar{D}^*\Sigma_c^*$	$\frac{3}{2}^-$	10.1 – 10.2	4516.5 – 4516.6
B	$\bar{D}^*\Sigma_c^*$	$\frac{5}{2}^-$	25.7 – 26.5	4500.2 – 4501.0

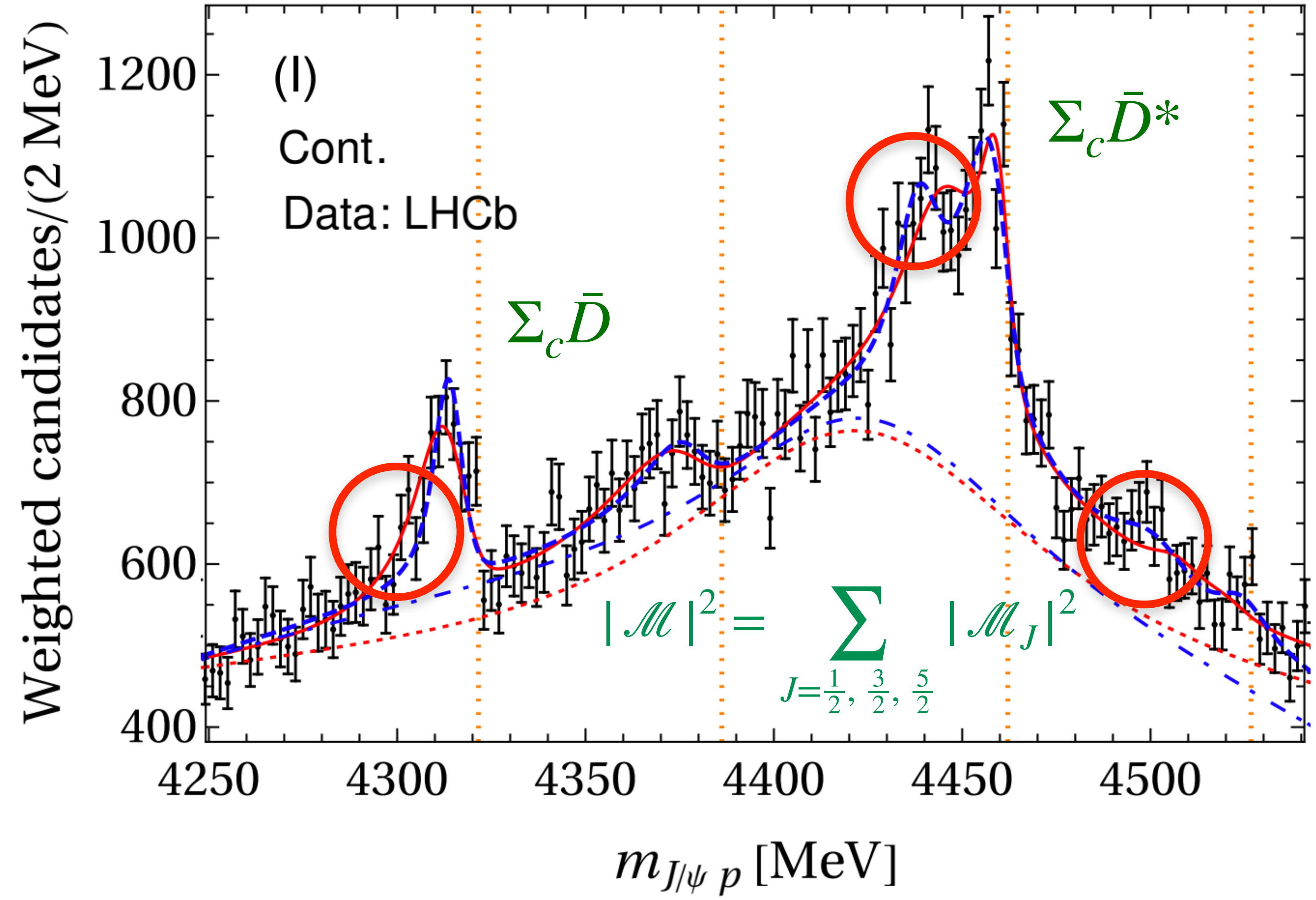

- Two parameters determined by

$P_c(4440),\ P_c(4457)$

- Two solutions

- Two parameters $g_S,\ g_D$ for $J/\psi p,\ \eta_c p$
- Predict pole positions accurately
- $\chi^2_A < \chi^2_B$
- The effect of each data point is different

Du, Baru, Guo, Hanhart, Meißner, Oller, **QW,** PRL124(2020)072001

Multi-channel case in 2023

The $\Sigma_c^{(*)}\bar{D}^{(*)}$ molecular picture

LHCb, PRL122(2019)222001

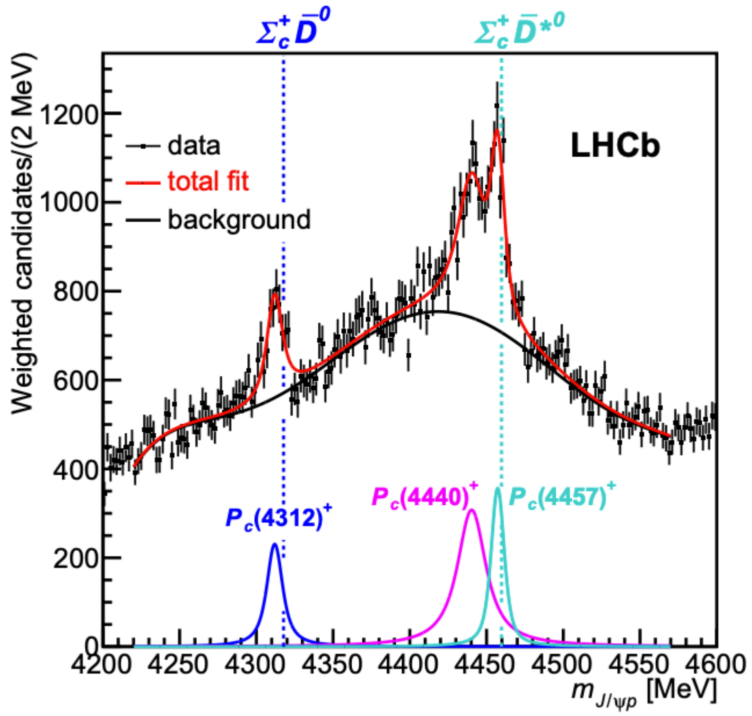

- $P_c(4312)$ bound state or virtual state?
- Spin assignment of $P_c(4440)$ and $P_c(4457)$?
- The pole situations for all the P_c states?
- Whether NN approach obtains more than the normal fitting approach?

LO HQEFT, **Du**, **Baru, Guo, Hanhart, Meißner**, Oller, **QW,** PRL124(2020)072001

The decay amplitude for $\Lambda_b \to J/\psi p K^-$ process

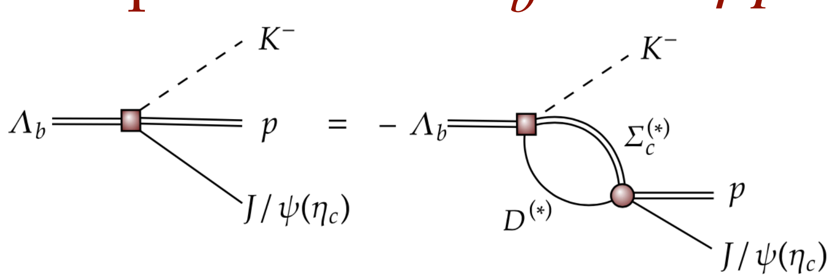

Zhang, Liu, Hu, **QW, Meißner**, Sci.Bull.68(2023)981-989

The decay amplitude for $\Lambda_b \to \Sigma_c^{(*)}\bar{D}^{(*)}K^-$ process

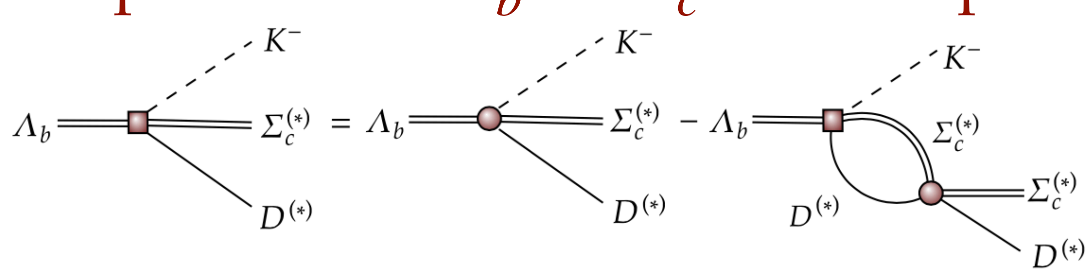

Multi-channel case in 2023

States for 3-channel case

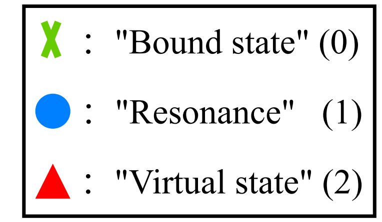

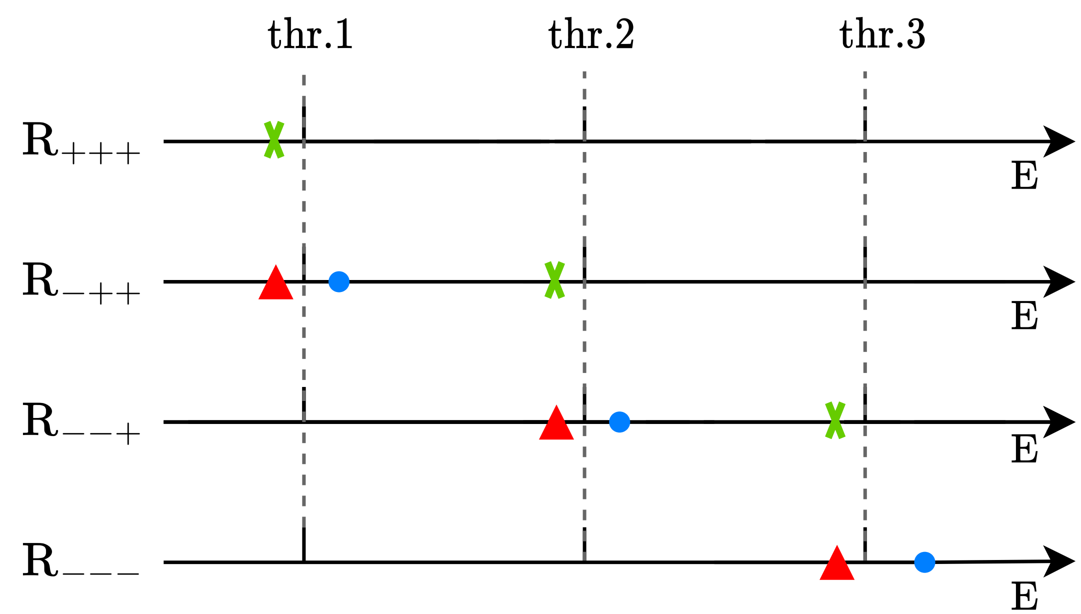

States and labels

- "+" and "-" for phy. and unphy. sheets
- $\frac{1}{2}^-$ dyn. Channels: $\Sigma_c\bar{D}$, $\Sigma_c\bar{D}^*$, $\Sigma_c^*\bar{D}^*$
- $\frac{3}{2}^-$ dyn. Channels: $\Sigma_c^*\bar{D}$, $\Sigma_c\bar{D}^*$, $\Sigma_c^*\bar{D}^*$
- $\frac{5}{2}^-$ dyn. Channel: $\Sigma_c^*\bar{D}^*$

States for 1-channel case

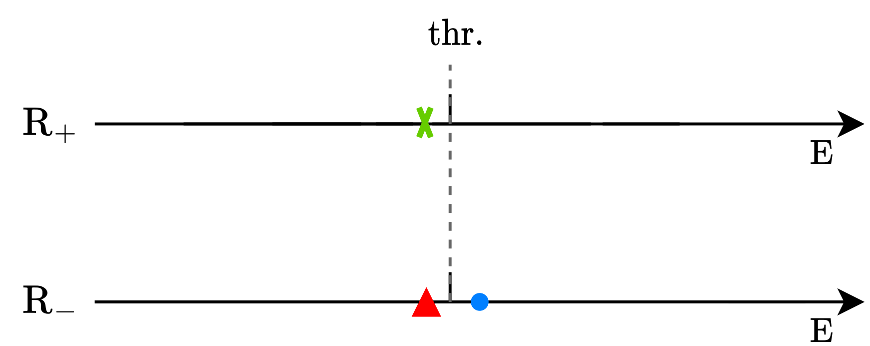

LHCb, PRL122(2019)222001

Bound state for $J = \frac{1}{2}, \frac{3}{2}, \frac{5}{2}$ channels

Solution B 0000

Zhang, Liu, Hu, **QW, Meißner**, Sci.Bull.68(2023)981-989

- Mass label 1 and 0 for $J_{P_c(4440)} = \frac{1}{2}, J_{P_c(4457)} = \frac{3}{2}$ and $J_{P_c(4440)} = \frac{3}{2}, J_{P_c(4457)} = \frac{1}{2}$,

i.e. solution A and B in PRL122(2019)242001, PRL124(2020)072001, JHEP08(2021)157

Multi-channel case in 2023

Training and verification

240184 samples

Mass Relation Label	State Label	Number of Samples
0	000	46951
1	000	4283
1	001	1260
1	002	4360
0	100	3740
0	110	4320
0	111	7520
1	111	360
0	200	9590
1	200	280
1	210	3980
1	211	2690
1	220	50240
1	221	50512
1	222	50098

Predicted probability

Output(%) Label / NN	0000	1000	1001	1002	100X	others
prediction of NN trained with $\{S^{90}\}$ samples.						
NN 1	0.69	89.13	1.42	8.75	99.30	0.01
NN 2	0.03	5.83	38.47	55.30	99.60	0.37
NN 3	0.03	5.39	15.79	78.41	99.59	0.11
NN 4	0.01	1.9	27.01	70.95	99.86	0.13
NN 5	2.40	94.45	0.15	2.99	97.59	0.01
5 NNs Average	0.63(1.03)	39.34	16.57	43.28	99.19(0.91)	0.13(0.15)
10 NNs Average	0.36(0.74)	21.16	20.69	57.62	99.47(0.68)	0.12(0.13)
prediction of NN trained with $\{S^{92}\}$ samples.						
NN 1	0.00	0.15	5.37	94.47	99.99	0.00
NN 2	0.00	0.07	4.11	95.81	99.99	0.00
NN 3	0.00	0.78	13.57	85.61	99.96	0.03
NN 4	0.00	0.81	19.02	80.16	99.99	0.00
NN 5	0.14	15.13	16.91	67.80	99.84	0.00
5 NNs Average	0.03(0.06)	3.39	11.80	84.77	99.95(0.06)	0.01(0.01)
10 NNs Average	0.01(0.04)	1.78	9.50	88.70	99.97(0.04)	0.00(0.01)

- 5 and 10 NN models with an identical structure under different initialization
- The uncertainties decrease with the increasing number of NNs
- Top 3 probabilities, 1000,1001,1002 favor solution A
- Bound states in $J^P = \frac{1}{2}^-, \frac{3}{2}^-$ channels, Undetermined for $J^P = \frac{5}{2}^-$ channel
- The NNs successfully retrieve the state label with an accuracy (standard deviation) of

75.91(1.18) %, 73.14(1.05) %, 65.25(1.80) %, 54.35(2.32) % for the samples $\{\mathcal{S}^{90}\}, \{\mathcal{S}^{92}\}, \{\mathcal{S}^{94}\}, \{\mathcal{S}^{96}\}$

Zhang, Liu, Hu, **QW, Meißner**, Sci.Bull.68(2023)981-989

Multi-channel case in 2023

Why NN favors Solution A?

Generate 100 1xxx samples and 100 0xxx samples

Reduced chisq from the normal fitting

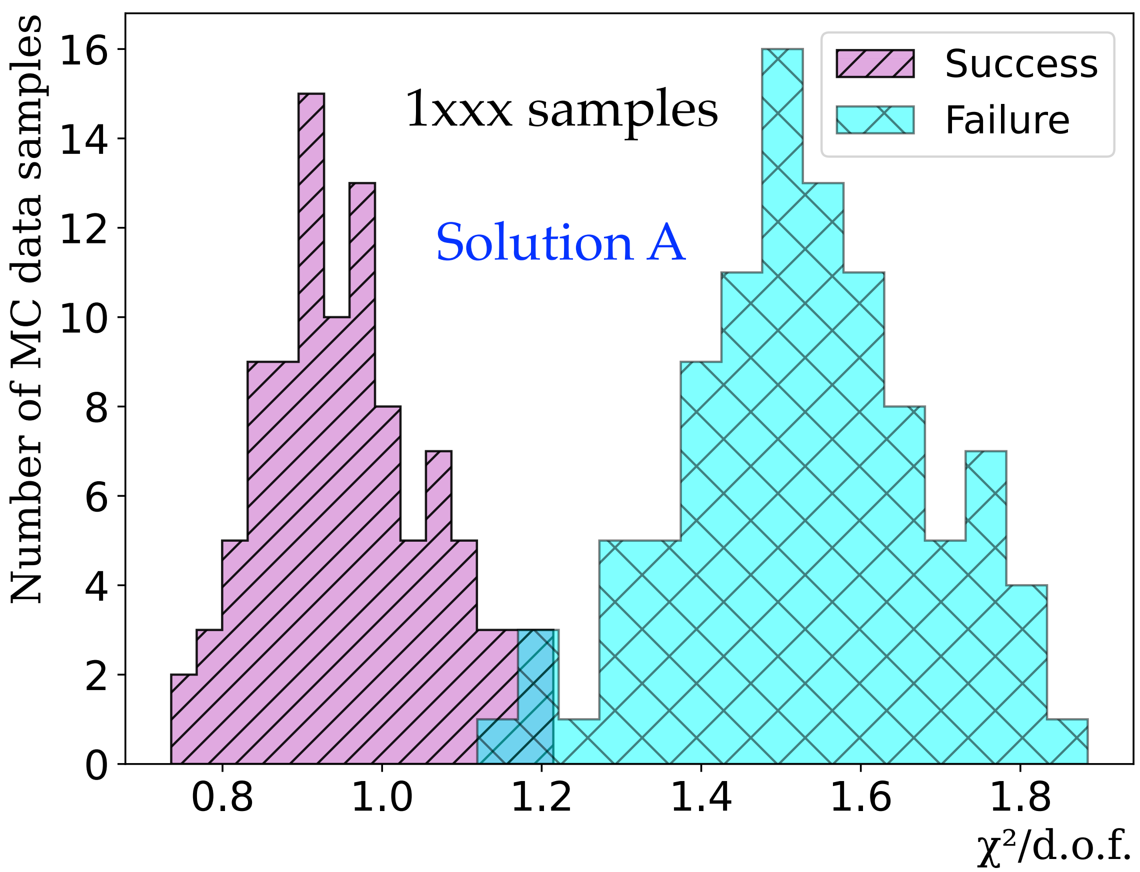

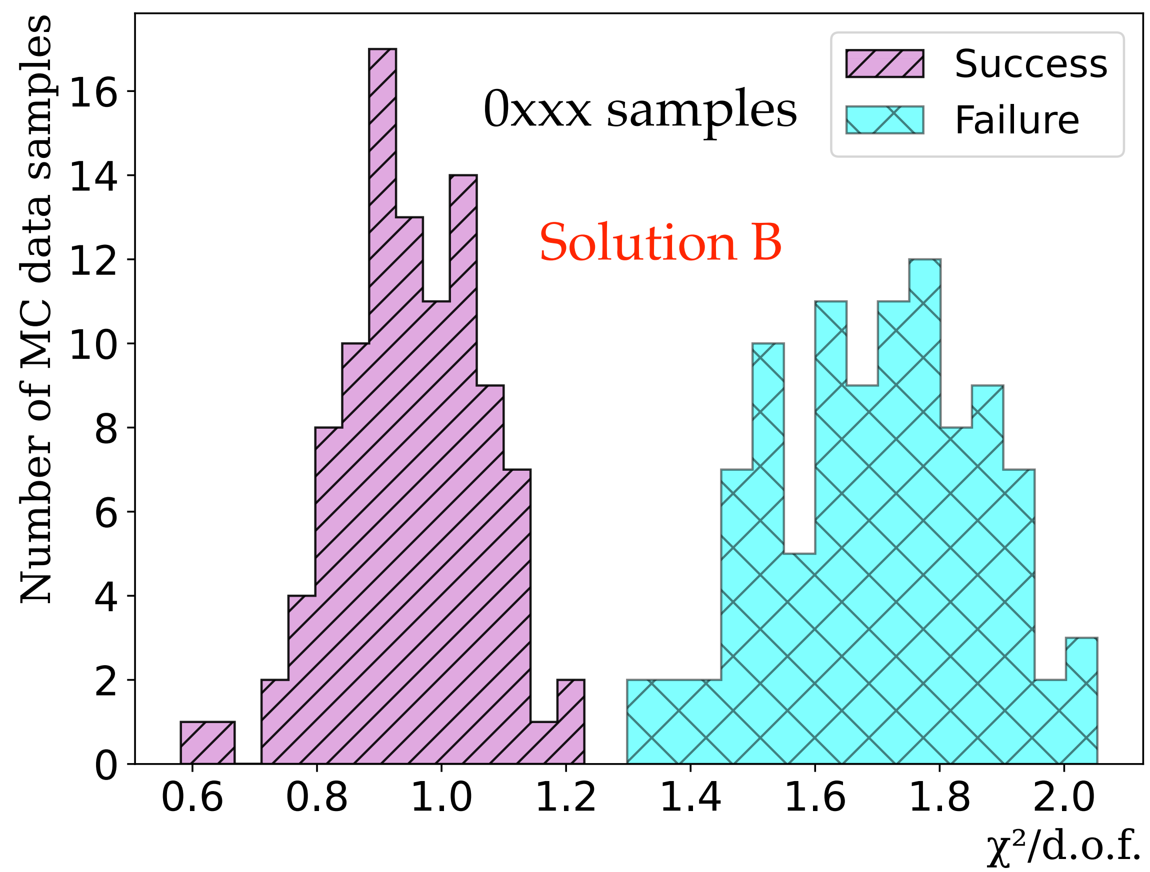

- A 3% misidentification for 1xxx samples

Zhang, Liu, Hu, **QW, Meißner**, Sci.Bull.68(2023)981-989

Multi-channel case in 2023

Why NN favors Solution A?

Generate 100 1xxx samples and 100 0xxx samples

Probabilities from NN

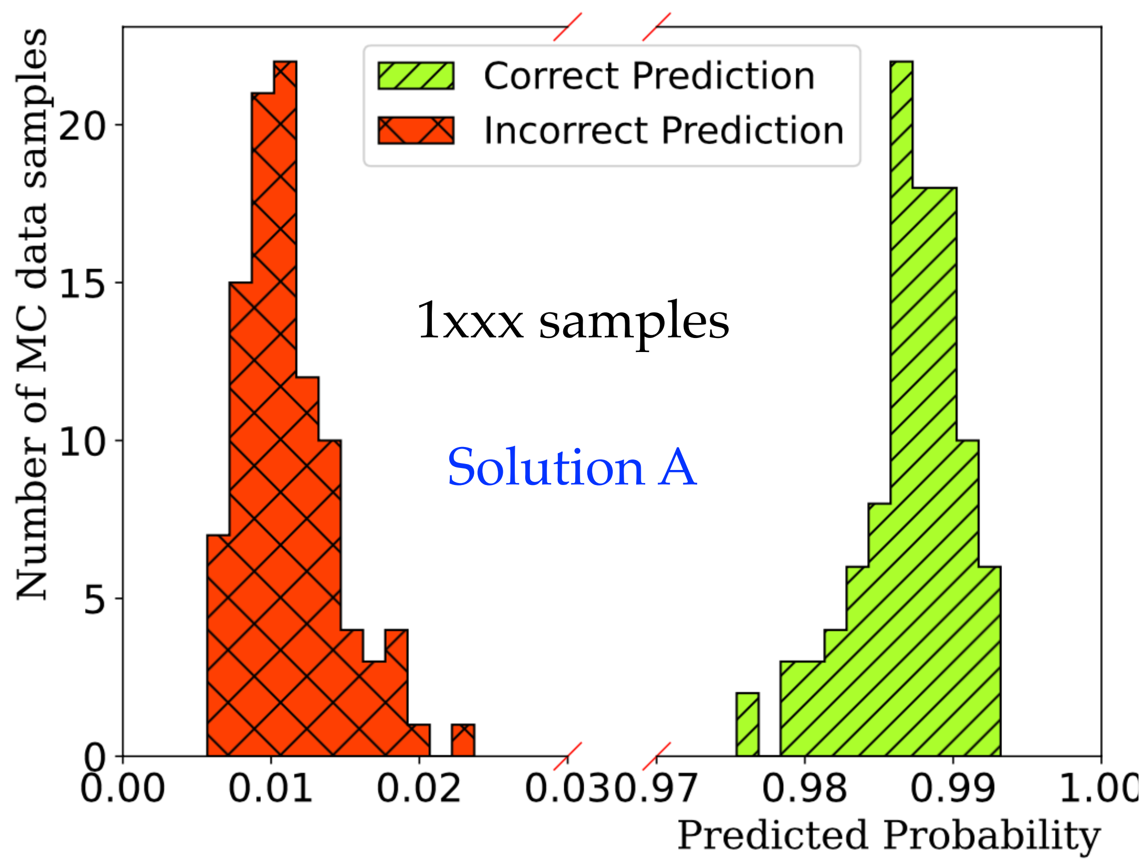

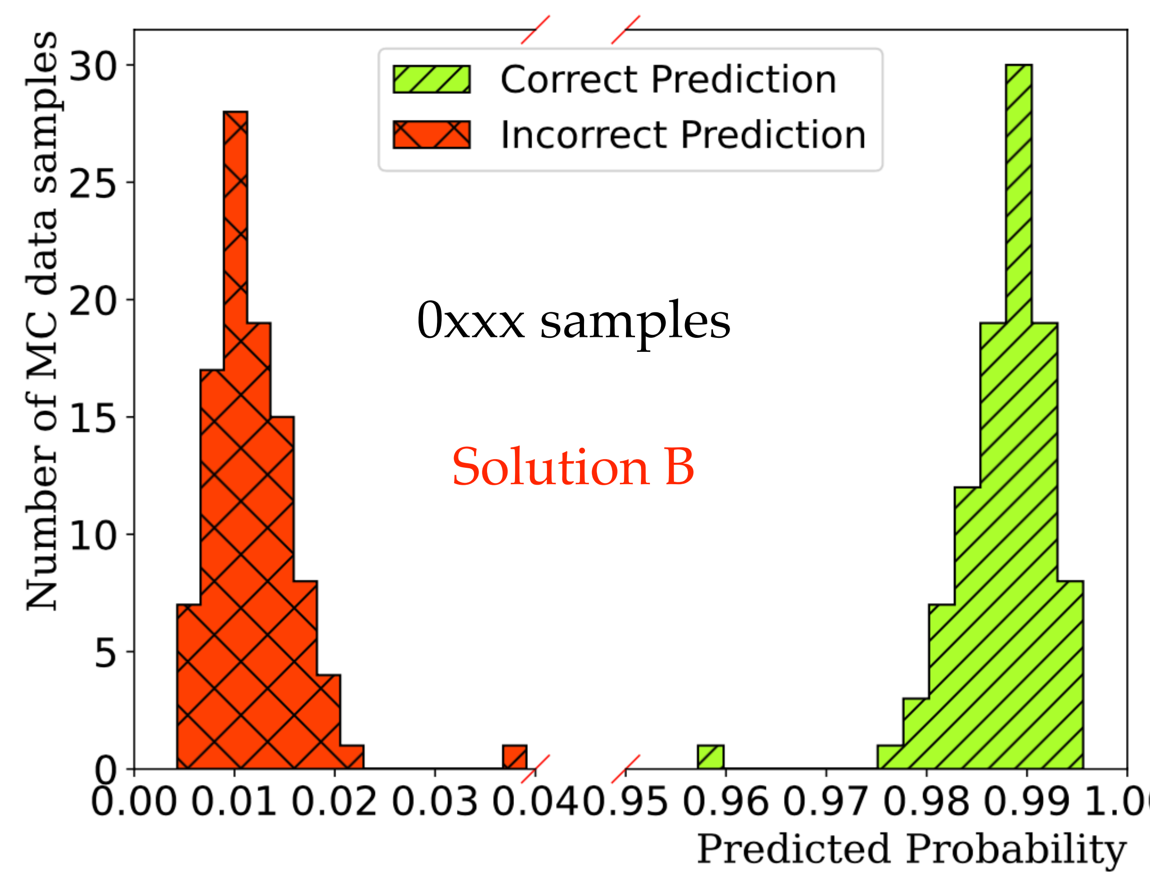

- The NN can make a good prediction
- The two solutions are well distinguished for both samples

Zhang, Liu, Hu, **QW, Meißner**, Sci.Bull.68(2023)981-989

Multi-channel case in 2023

The impact of each experimental data point in NN

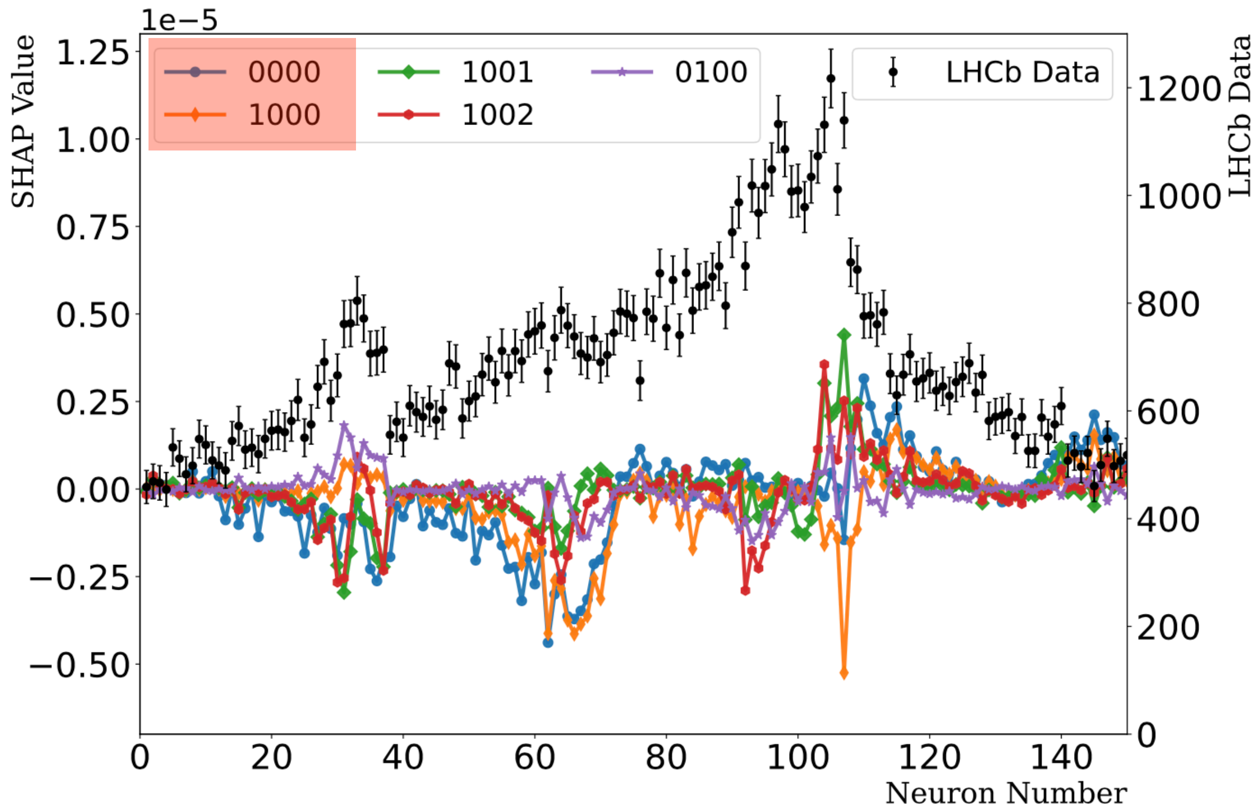

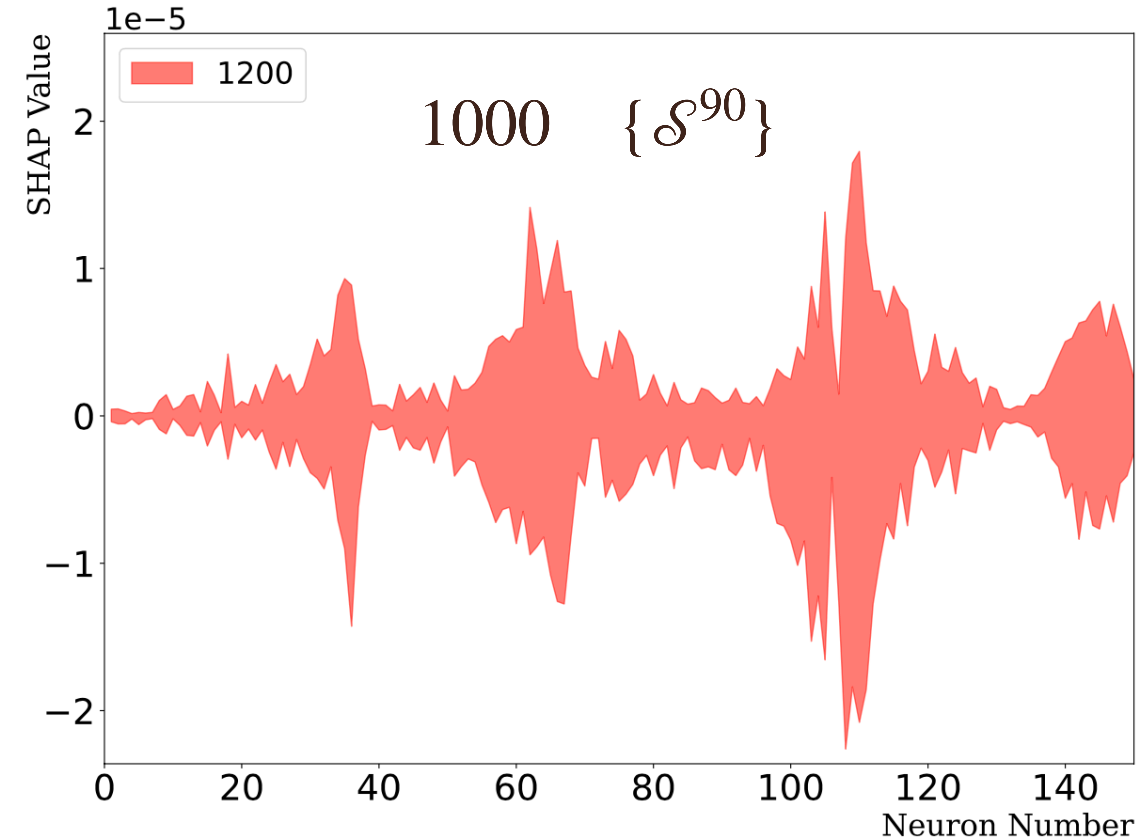

- The Shapley Additive exPlanation (SHAP) is investigated.
- A positive (negative) SHAP value indicates that a given data point is pushing the NN classification in favor of (against) a given class.
- The data points around the peaks in the mass spectrum have a greater impact.

Zhang, Liu, Hu, **QW, Meißner,** Sci.Bull.68(2023)981-989

Multi-channel case in 2023

The impact of each experimental data point in NN

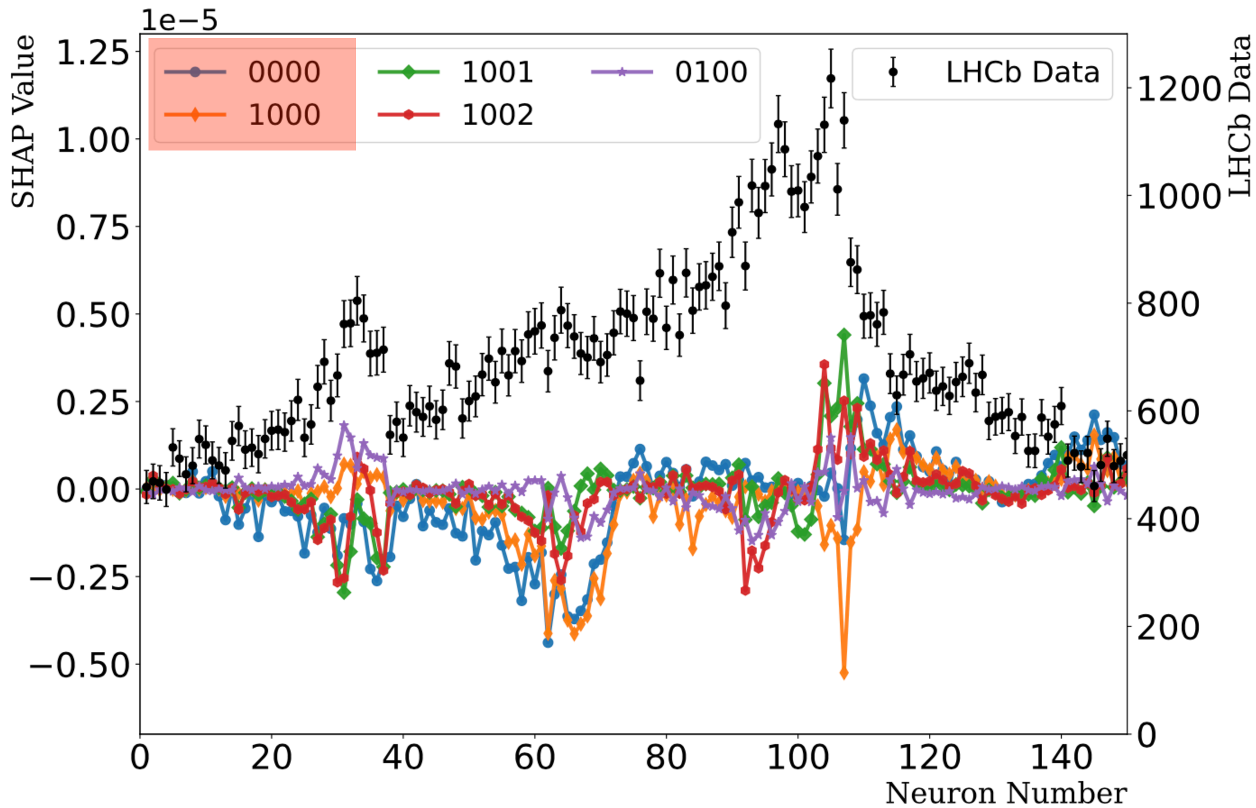

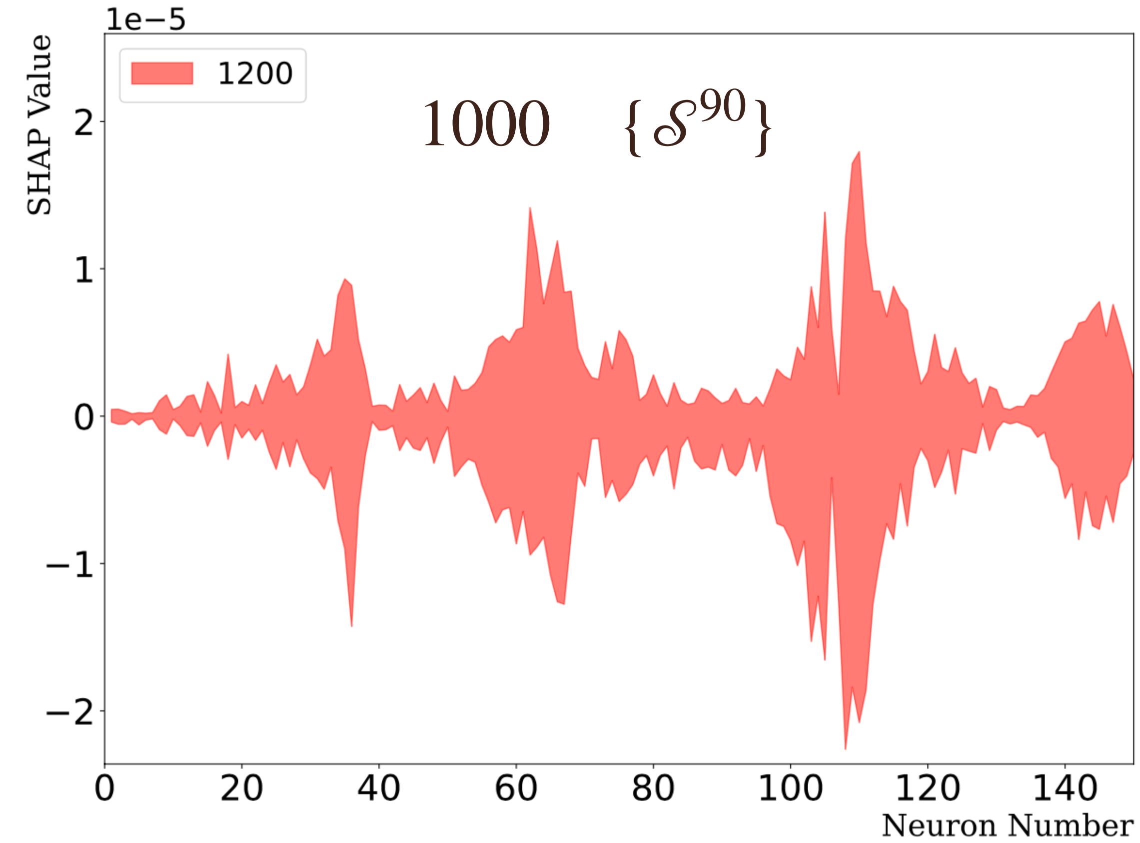

- The Shapley Additive exPlanation (SHAP) is investigated.
- A positive (negative) SHAP value indicates that a given data point is pushing

ML can extract more information than normal fitting approach

Zhang, Liu, Hu, **QW, Meißner,** Sci.Bull.68(2023)981-989

Three-body system on the lattice in 2024

Many-body system

Science

Current Issue   First release papers   Archive   About   Submit manuscript

HOME > SCIENCE > VOL. 177, NO. 4047 > MORE IS DIFFERENT

ARTICLE

More Is Different: Broken symmetry and

P. W. ANDERSON   Authors Info & Affiliations

SCIENCE • 4 Aug 1972 • Vol 177, Issue 4047 • pp. 393-396 • DOI: 10.1126/science.177.404

Three ways to decipher the nature of exotic hadrons: Multiplets, three-body hadronic molecules, and correlation functions #52

Ming-Zhu Liu (Lanzhou U. (main)), Ya-Wen Pan (Beihang U.), Zhi-Wei Liu (Beihang U.), Tian-Wei Wu (SYSU, Guangzhou), Jun-Xu Lu (Beihang U.) et al. (Apr 9, 2024)

Published in: *Phys.Rept.* 1108 (2025) 1-108 • e-Print: 2404.06399 [hep-ph]

pdf   DOI   cite   claim   reference search   71 citations

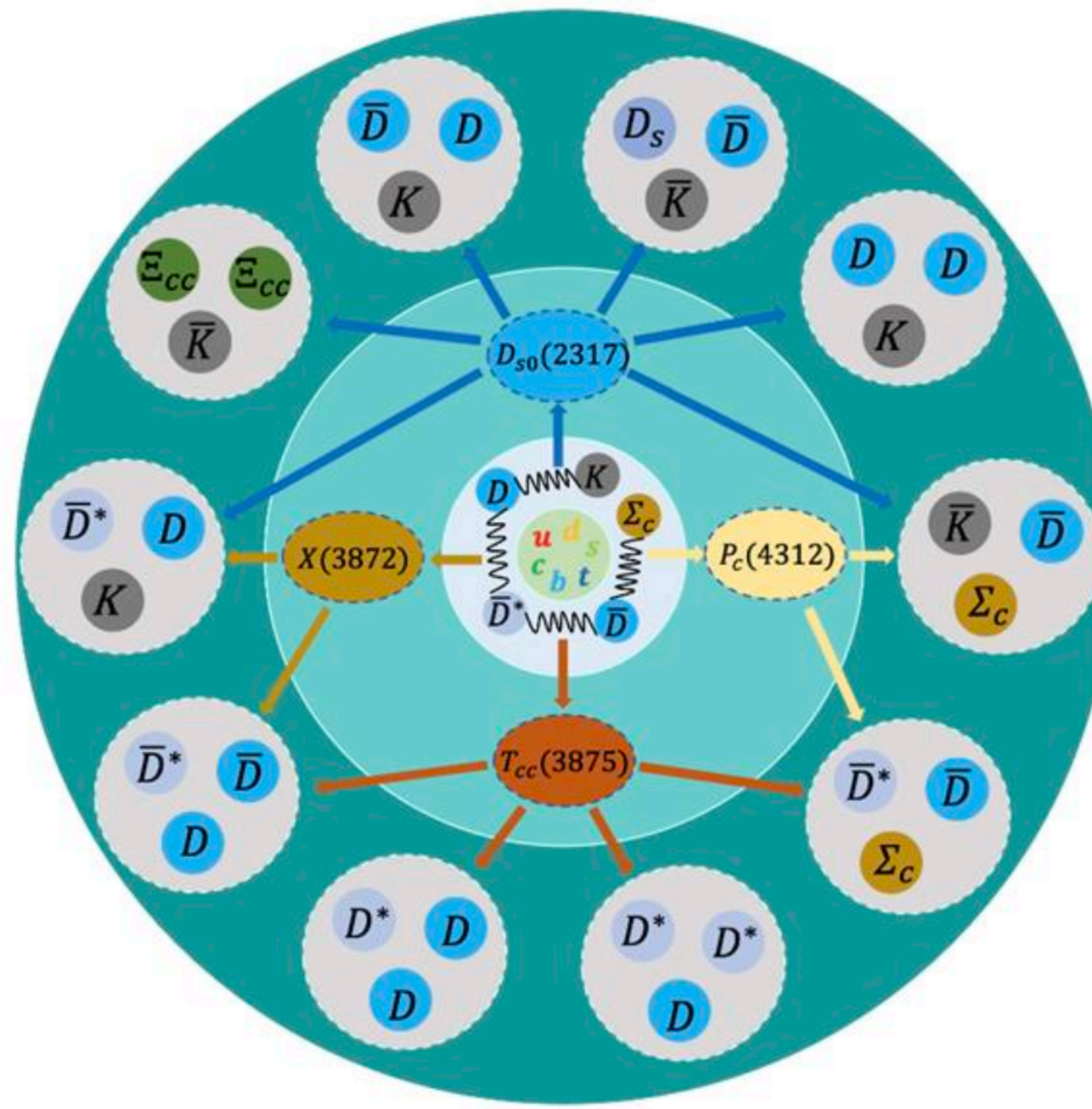

E. Oset, T. Hyodo, K.P. Khemchandani, A. Martinez Torres, L.S. Geng, C.W. Xiao, M.P. Valderramma, A. Hosaka, F.K. Guo……

Liu et al., Phys.Rept.1108(2025)1   Wu et al., Sci.Bull.67(2022)1735-1738

Three-body system on the lattice in 2024

Applications in Hadron Physics

TABLE XXXIX. Summary for heavy-flavor three-body states. Energies are in units of MeV.

Components	$I(J^P)$	Results (Method)	Decay modes
DNN	$\frac{1}{2}(0^-)$	BS $\sim 3500 - 15i$ (FCA, V) [836]	$\Lambda_c\pi^- p, \Lambda_c p$ [836]
$NDK, ND\bar{K}, ND\bar{D}$	$\frac{1}{2}(\frac{1}{2}^+)$	BS $\sim 3050, 3150, 4400$ (FCA) [837]	†
DD^*N	$\frac{1}{2}(\frac{1}{2}^+, \frac{3}{2}^+)$	BS $\sim 4773.2, 4790.7$ (GEM) [838]	$T_{cc}p, DDp + \pi(\gamma), \Xi_{cc} + \pi(\gamma)$, charmed baryon + charmed meson [838]
DD^*N	$\frac{3}{2}(-)$	difficult to form bound states (GEM) [838]	†
$DK\bar{K}$	$\frac{1}{2}(0^-)$	D-like state ~ 2845.5 (FCA) [821], D-like state ~ 2900 (QCDSR, χF) [839]	$\pi\pi D$ [821]
DKK	$\frac{1}{2}(0^-)$	no bound state (FCA) [821]	†
$\bar{D}\bar{K}\Sigma_c$	$1(\frac{1}{2}^+)$	BS ~ 4738.6 (GEM) [840]	$D\Xi', D_s\Sigma_c$ [840]
$D^{(*)}$ multi ρ	...	several $D_J^{(*)}$ states (FCA) [841, 842]	†
$\rho D\bar{D}$	$0(?), 1(?)$	BS $\sim 4241 - 10i, [4320 - 13i, 4256 - 14i]$ (FCA) [843]	†
DDK	$\frac{1}{2}(0^-)$	BS ~ 4162 (GEM) [273], 4140 (χF) [819], 4160 (FV) [820]	DD_s^*, D^*D_s [826]
$D\bar{D}K$	$\frac{1}{2}(0^-)$	BS ~ 4181.2 (GEM) [822], 4191 (FCA) [825]	$D_s\bar{D}^*, J/\psi K$ [822]
DD^*K	$\frac{1}{2}(1^-)$	BS ~ 4317.9 (BO) [823]	†
$D\bar{D}^*K$	$\frac{1}{2}(1^-)$	BS ~ 4294.1 (GEM) [822], 4317.9 (BO) [823], 4307 (FCA) [824]	$D_s^{(*)}\bar{D}^{(*)}, J/\psi K^*$ [823, 844]
$D^*D^*\bar{K}^*$	$\frac{1}{2}(0^-, 1^-, 2^-)$	$4845 - 40i$, BS $\sim [4850 - 46i, 4754 - 50i]$, (FCA) [845] $[4840 - 43i, 4755 - 50i]$	$D^*D^*\bar{K}^*$, $D^*D^{(*)}\bar{K}^*$, $[D^*D^*\bar{K}^*, D^*D^{(*)}\bar{K}^*]$ [845]
$\bar{D}\bar{D}^*\Sigma_c$	$1(\frac{1}{2}^+, \frac{3}{2}^+)$	BS $\sim 6292.3, 6301.5$ (GEM) [829]	$J/\psi p\bar{D}^{(*)}, \bar{T}_{cc}\Lambda_c\pi$ [829]
$J/\psi K\bar{K}$	$0(1^-)$	$Y(4260) \sim 4150 - 45i$ (χF) [481]	†
DDD^*	$\frac{1}{2}(1^-)$	BS ~ 5742.2 (GEM) [833]	$DDD\pi(\gamma)$[833]
DD^*D^*	$\frac{1}{2}(0^-, 1^-, 2^-)$	several loosely bound states (GEM) [834]	charmed mesons + ... [834]
$D^*D^*D^*$	$\frac{1}{2}(0^-, 1^-, 2^-, 3^-)$; $\frac{1}{2}(0^-, 1^-, 2^-)$	several loosely bound states (GEM)[834]; BS $\sim 5790.9 - 49.8i, 5990.2, 5989.4$ (FCA) [835]	charmed mesons + ... [834]
$D^*D^*D^{(*)}$	$\frac{3}{2}(-)$	difficult to form bound states (GEM) [834]	†
$D^*D^*\bar{D}$	$\frac{1}{2}(2^-)$	BS ~ 5879 (F) [846]	†
$D^*D^*\bar{D}^*$	$\frac{1}{2}(3^-)$	BS ~ 6019 (F) [846]	†
$\Omega_{ccc}\Omega_{ccc}\Omega_{ccc}$	$?(\frac{3}{2}^+)$	no bound state (GEM) [847]	†
$\Xi_{cc}\Xi_{cc}\bar{K}$	$\frac{1}{2}(0^-)$	BS ~ 7641.8 (GEM) [848]	†

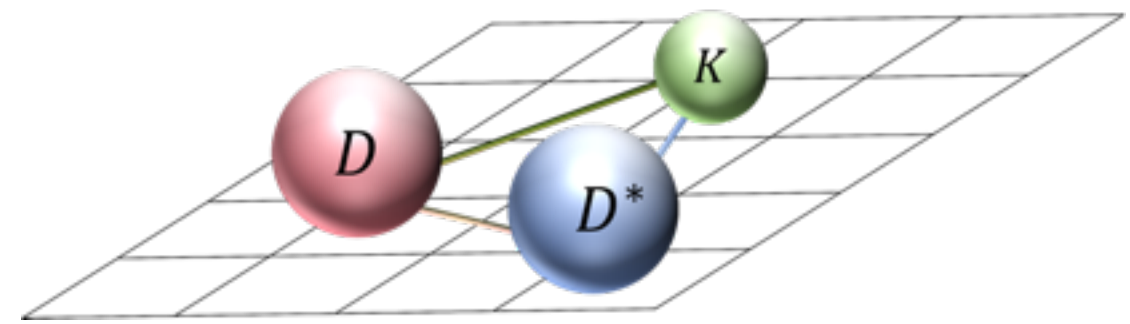

- Gaussian expansion method (GEM)
- QCD sum rule (QCDSR)
- Born-Oppenheimer approximation
- Fixed center approximation (FCA)
- Faddeev equation (F)

Without 3-body force!

Liu et al., Phys.Rept.1108(2025)1

Three-body system on the lattice in 2024

- The observation of $T_{cc}^{+}, D_{s0}^{*}(2317), D_{s1}(2460)$ in experiment

  - DD^{*} interaction: LO+OPE

    Du et al, PRD105(2022)014024

  - DK interaction: LO+NLO

    Guo et al, EPJA40(2009)171

  - $D^{*}K$ interaction: LO+NLO

  - Single particle regulator is used to obtain a better ren. Group invariant

Lu et al, arXiv:2308.14559

Three-body system on the lattice in 2024

Two-body parameters

$T_{cc}^{+} \Rightarrow v_0$ $\qquad D_{s0}^{*}(2317) \Rightarrow h_3$ $\qquad D_{s1}(2460) \Rightarrow h_3^{*}$

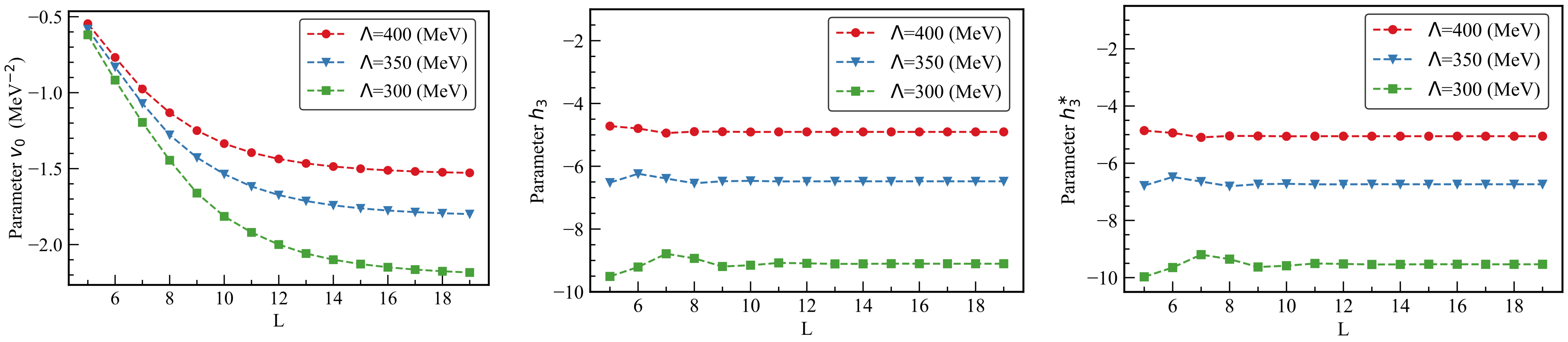

- Cubic lattice $L^3 = 5^3 \cdots 19^3$
- Cutoff $\Lambda = 300,\ 350,\ 400$ MeV in the regulator
- Lattice spacing $a = 1/200$ MeV ~ 0.99 fm
- v_0 converges slow $\Leftarrow$ long-ranged force+shallow bound state
- $\Lambda = 400$ MeV converges quickly

Zhang et al., Phys.Rev.D111(2025)036002

Three-body system on the lattice in 2024

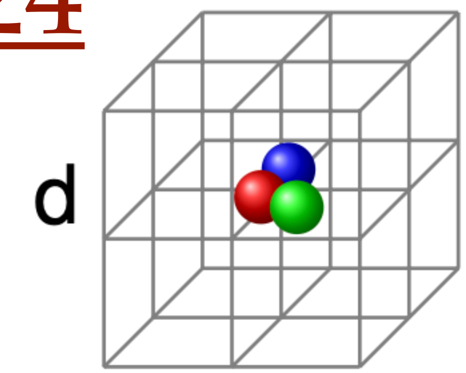

From Serdar's talk

Three-body interaction

- DD^*K Lag. $\mathscr{L} = c_3 \left\langle H\mathscr{D}_\mu H^\dagger H \mathscr{D}^\mu H^\dagger \right\rangle + c_3' \left\langle H\mathscr{A}_\mu H^\dagger H \mathscr{A}^\mu H^\dagger \right\rangle$

- DD^*K three-body force

$$V_{DD^*K}(p_i) = \frac{c_3}{4f_\pi^2}\left(p_1\cdot p_3 + p_1\cdot p_3' + p_2\cdot p_3 + p_2\cdot p_3' + p_1'\cdot p_3 + p_1'\cdot p_3' + p_2'\cdot p_3 + p_2'\cdot p_3'\right)\epsilon\cdot\epsilon^*$$

- DD^*K binding energy

Zhang et al., Phys.Rev.D111(2025)036002

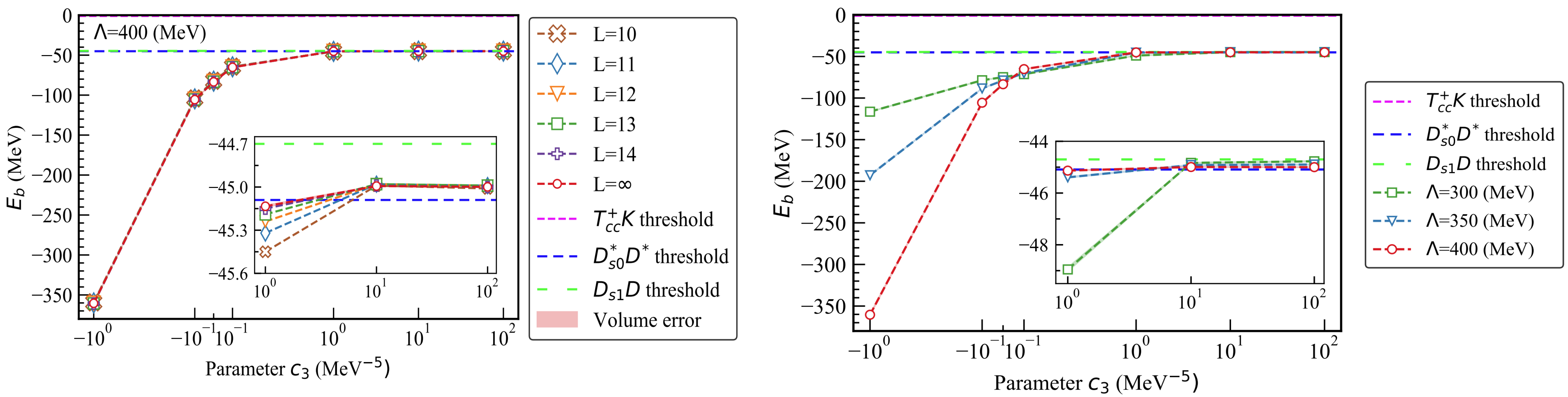

- Extrapolate to infinite volume

Meng et al., PRD98(2018)014508

$$\frac{\Delta E}{E_T} = -(\kappa L)^{-3/2}\sum_{i=1}^{3} C_i \exp\left(-\mu_i \kappa L\right)$$

- Switch off three-body force, the result is consistent with that in

Ma et al., CPC43(2019)014102

Three-body system on the lattice in 2024

The first excited states

- No experimental data ⇒ binding energy with $\Lambda = 400$ MeV as input
- The parameter c_3 at various cubic

Λ (MeV)	Parameter	L						State
		9	10	11	12	13	14	
400	c_3 (MeV^{-5})	0.100	0.100	0.100	0.100	0.100	0.100	Input
350		0.170	0.162	0.164	0.164	0.163	0.163	Fitted
300		0.328	0.305	0.281	0.278	0.281	0.280	Fitted

Zhang et al., Phys.Rev.D111(2025)036002

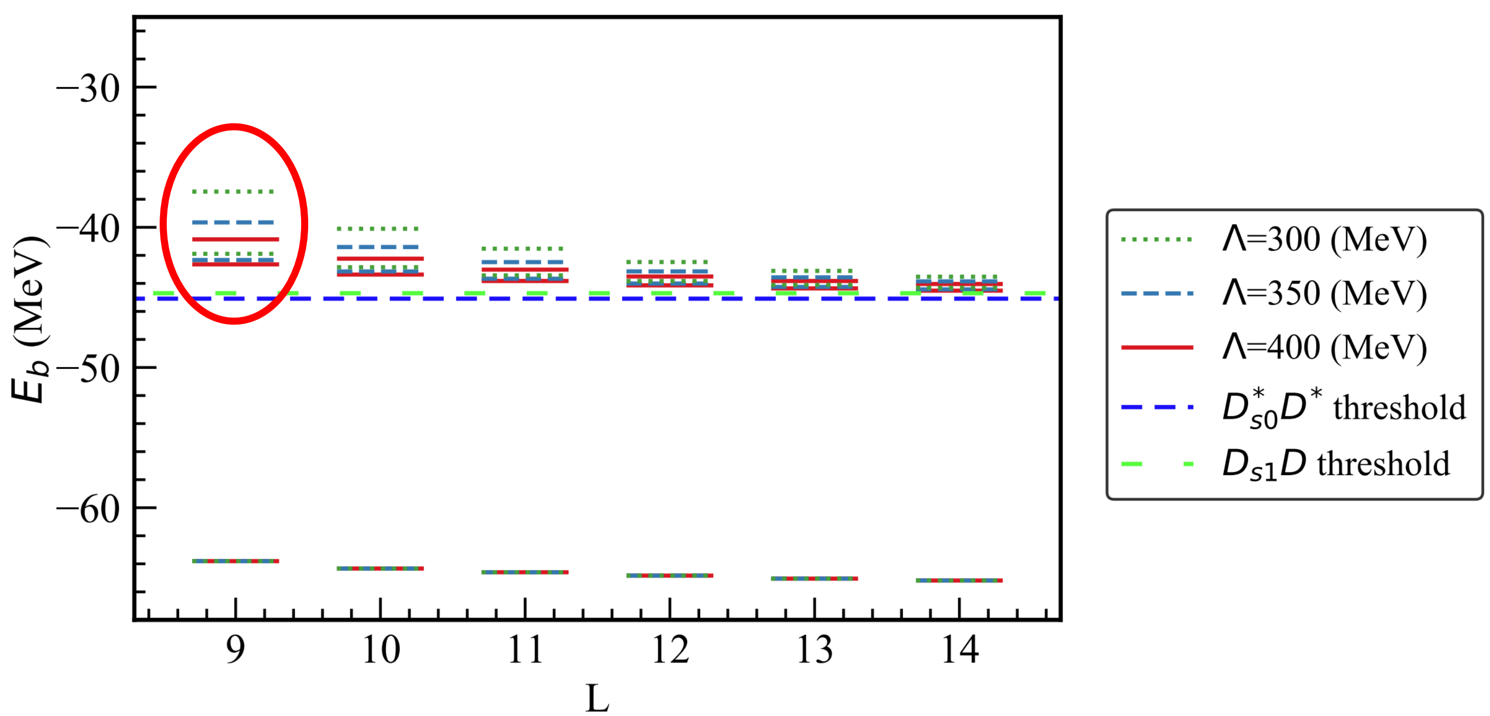

- $E^{\text{excited}}_{\Lambda_1} - E^{\text{excited}}_{\Lambda_2}$ decreases
- ρ-type and λ-type excitation
- The standard angular momentum and parity projection technique is used

- $J^P = 1^-$ $\Leftarrow$ $$\left|\Psi_A\right\rangle = \frac{d_n}{24}\sum_{i=1}^{24}\chi_n\left(\Omega_i\right)R\left(\Omega_i\right)\left|\Psi_0\right\rangle$$

Lu et al., PRD90(2014)034507

Three-body system on the lattice in 2024

$$\frac{\Delta E}{E_T} = -(\kappa L)^{-3/2} \sum_{i=1}^{3} C_i \exp\left(-\mu_i \kappa L\right)$$

Does this extrapolation formula also work for long-rang interaction?

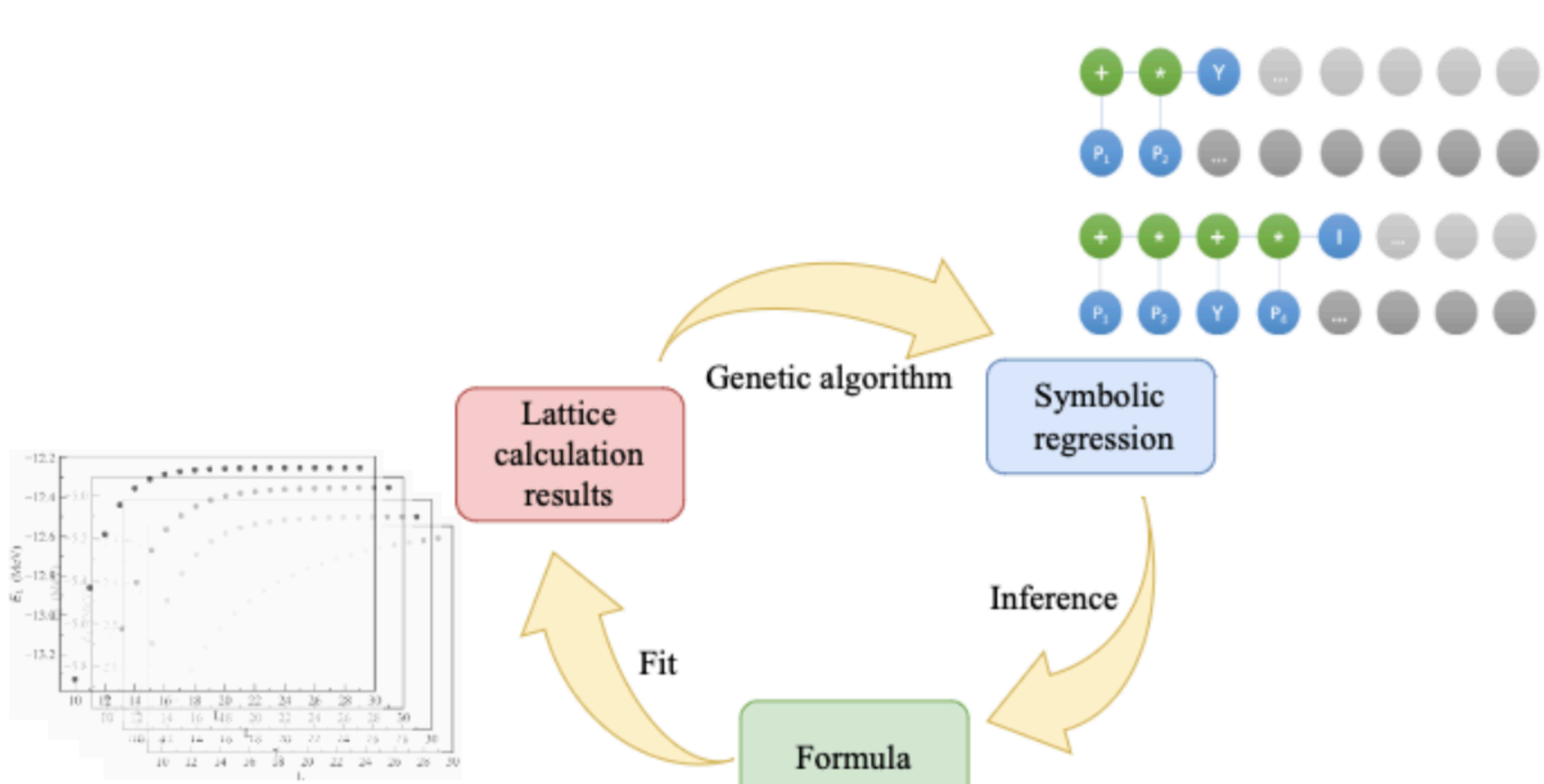

$$E_L = E_\infty + e^{-\kappa L}/L\ ?$$

Machine Learning Unveils the Power Law of Finite-Volume Energy Shifts,

9:40-10:00, 周日，张振宇

The power law of FV energy shift in 2025

The result of short-range interaction

- Box size 10 ~ 30 fm

$E_L = C_1 + C_2 e^{-C_3 L}/L^2$ (A)

$E_L = C_1 + C_2 e^{-C_3 L}/L$ (B)

$E_L = C_1 + C_2 e^{-C_3 L}$ (C)

- The value of C_3 is exactly the binding momentum

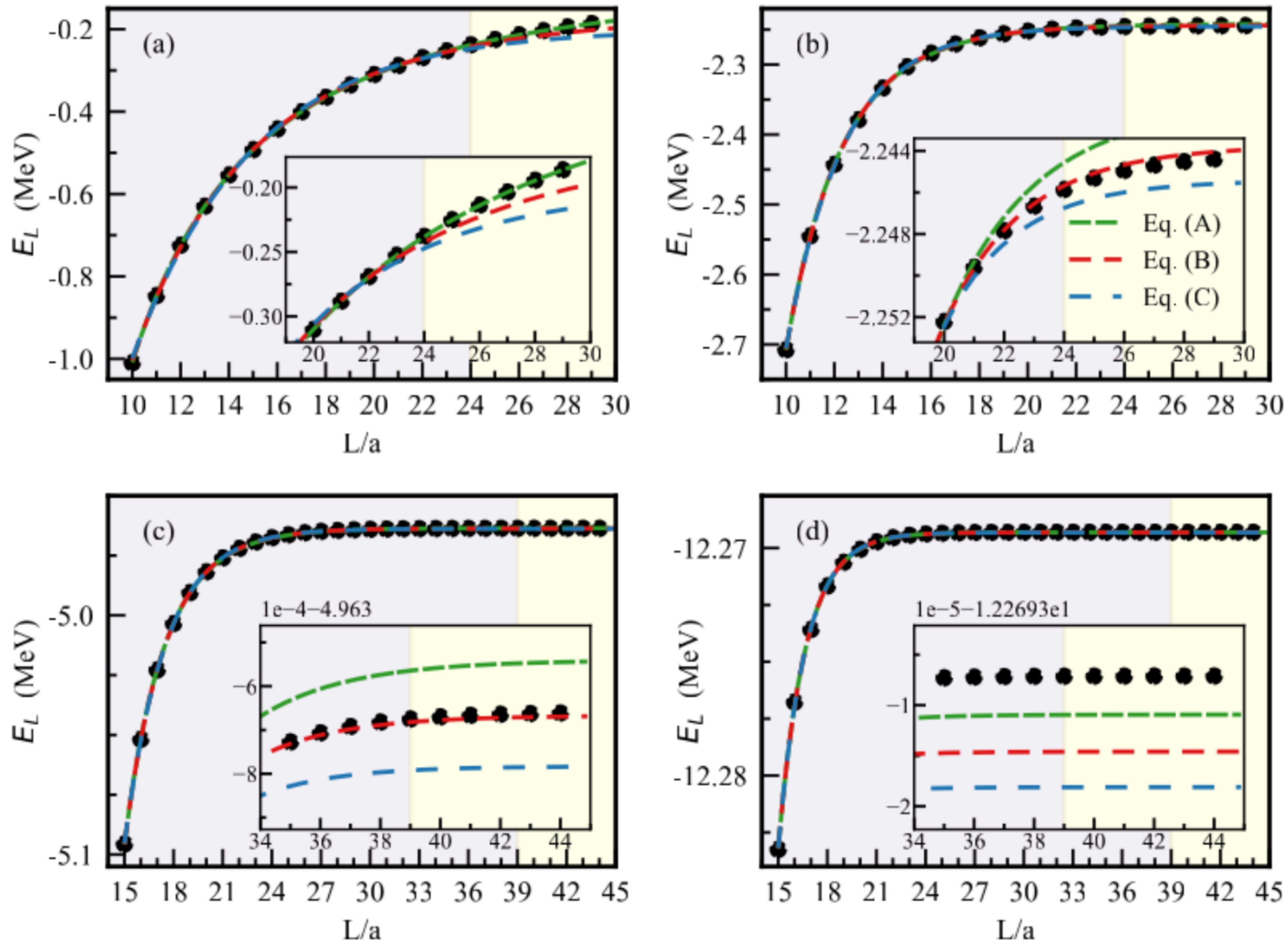

- Recover the formula of short-range interaction successfully

The power law of FV energy shift in 2025

The result of long-range interaction

- Box size $10 \sim 30$ fm

$$E_L = C_1 + C_2 e^{-C_3 L}/L \quad \text{(A)}$$

$$E_L = C_1 + C_2 e^{-C_3 L} \quad \text{(B)}$$

$$E_L = C_1 + C_2 e^{-C_3 L} L \quad \text{(C)}$$

- The power of L increases 2 for 10 fm range interaction

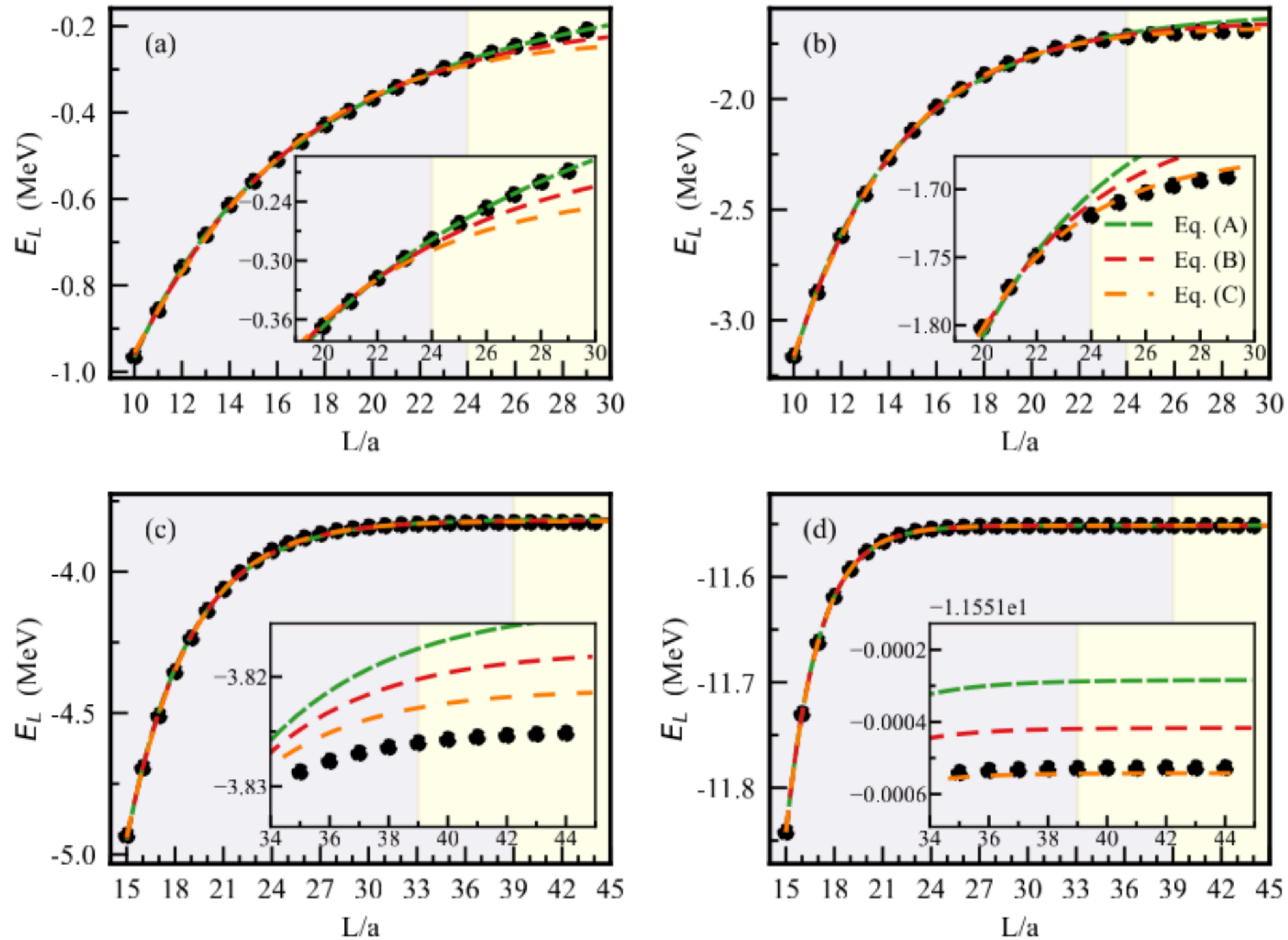

- The range parameter is set $\mu = 20$ MeV
- The power depends on the range of the force $E_L = C_1 + C_2 e^{-C_3 L} L^n$

The power law of FV energy shift in 2025

The n and C_3 value

$\mu = 10, 20, \ldots, 120, 400, 600, 800\text{MeV}$

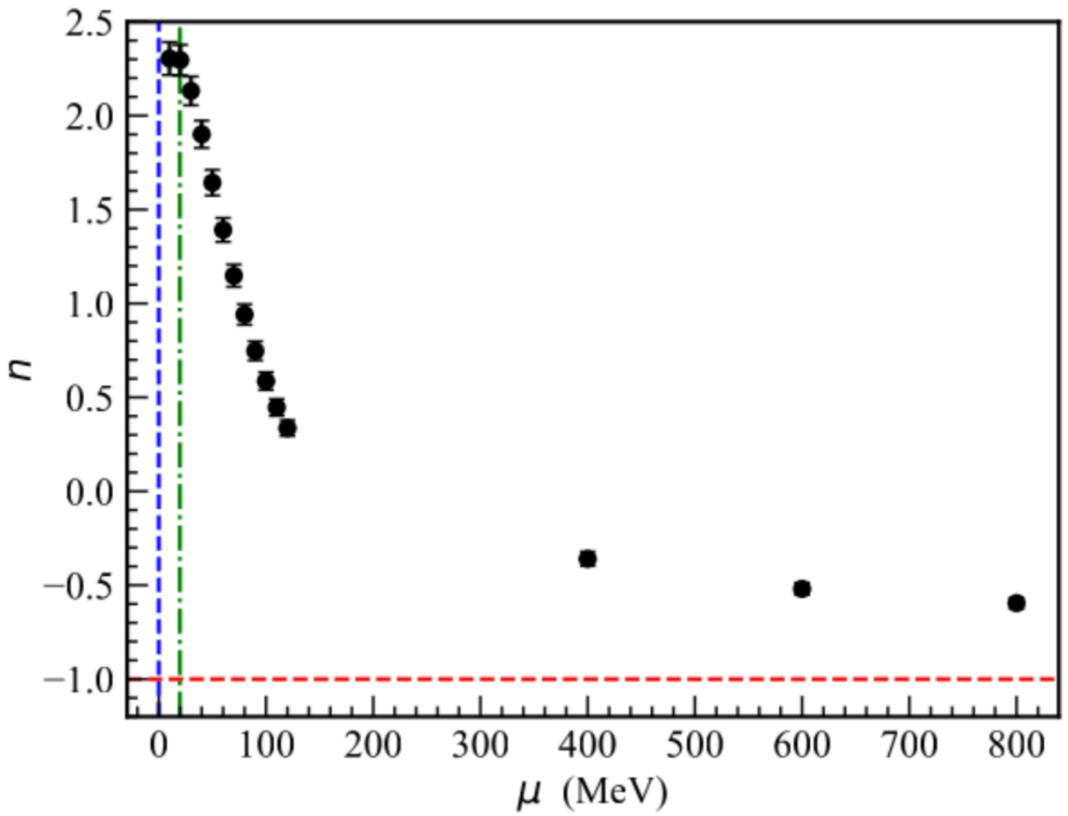

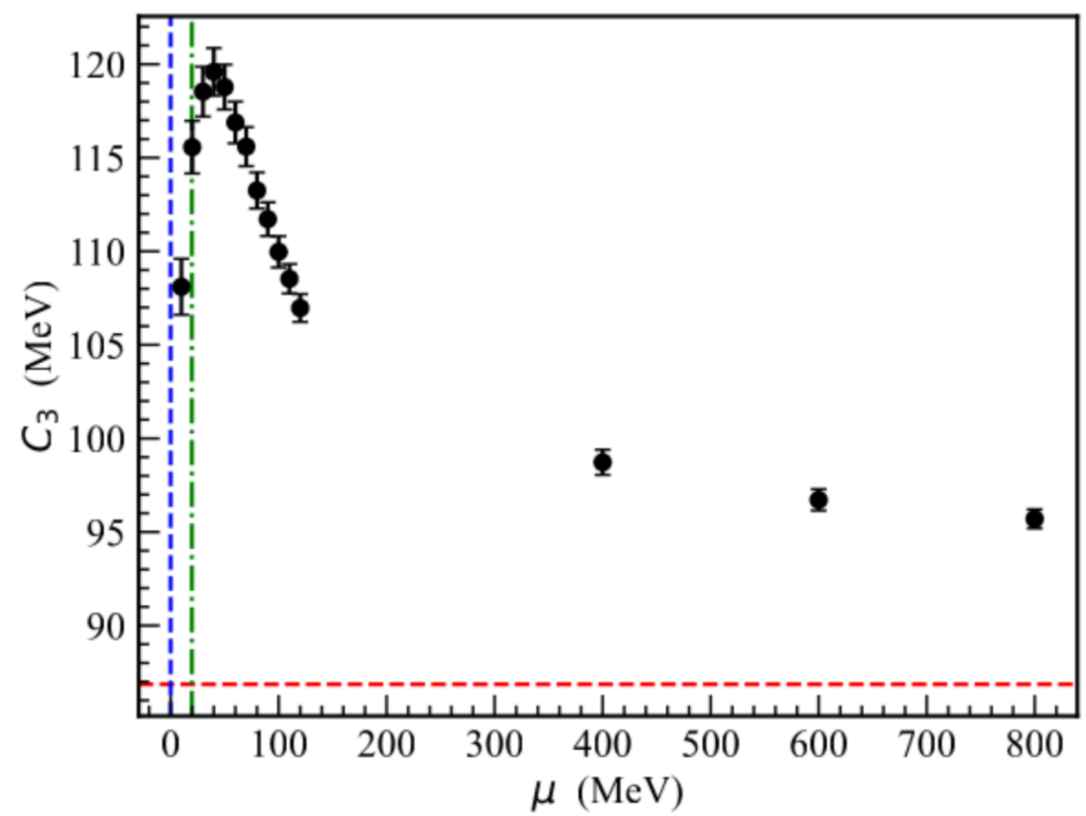

- $n = -1$
- $\mu = 0$
- $\hbar c / 10\ \text{fm} \sim 20\ \text{MeV}$

- κ_B
- $\mu = 0$
- $\hbar c / 10\ \text{fm} \sim 20\ \text{MeV}$

- The regressed formula recovers the short-range limit and indicates the long-range tendency

The power law of FV energy shift in 2025

The n and C_3 value

$\mu = 10,\ 20, \ldots,\ 120,\ 400,\ 600,\ 800\text{MeV}$

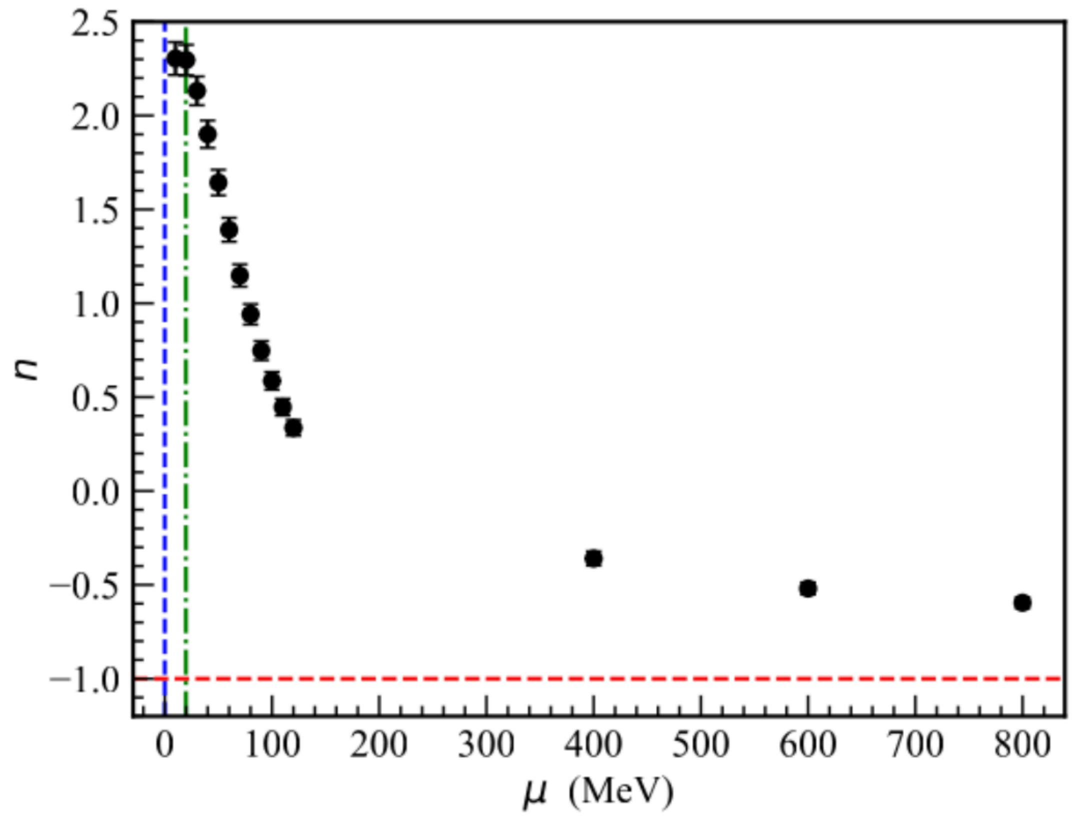

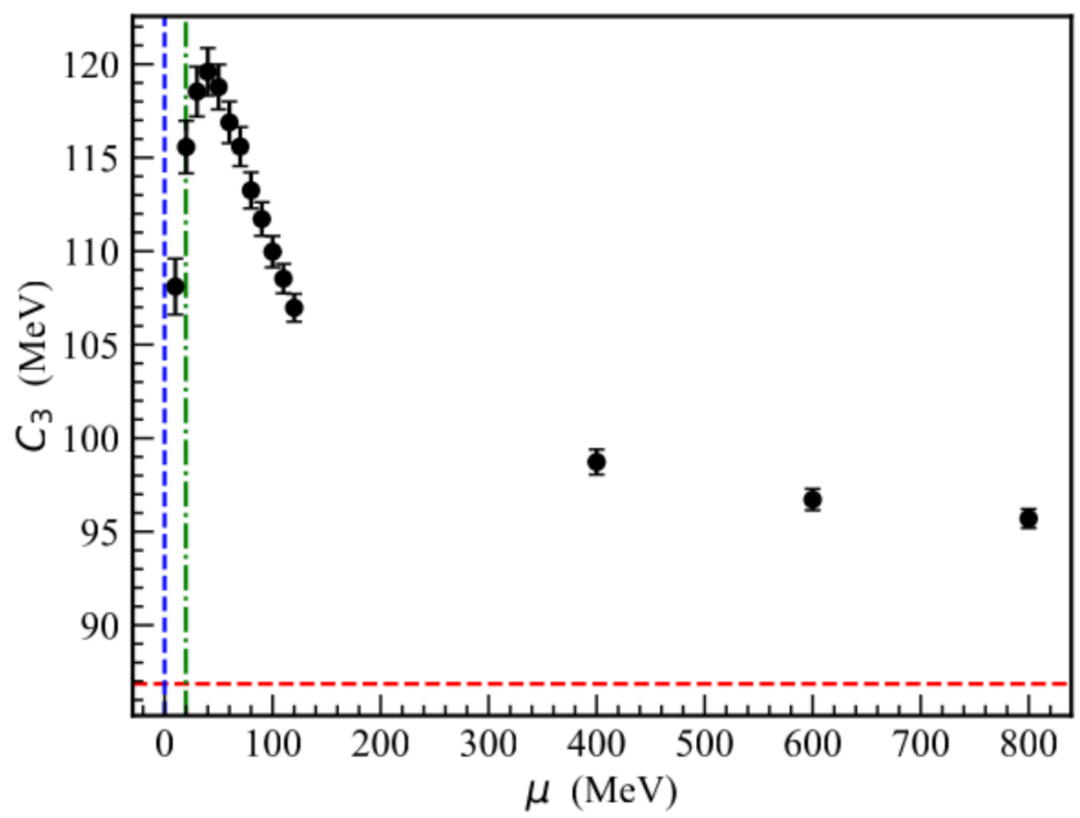

- $n = -1$
- $\mu = 0$
- $\hbar c/10\text{ fm} \sim 20\text{ MeV}$

- κ_B
- $\mu = 0$
- $\hbar c/10\text{ fm} \sim 20\text{ MeV}$

The ML can extract unknown formula!

Summary and outlook

2022 One-channel analysis

ML can do as good as normal fitting approach

2023 Multi-channel analysis ⇒ ML can extract more information

ML can extract more information than normal fitting approach

2025 Power law of FV energy shift ⇒ ML can extract unknown formula

Avoid model dependence.

XXXX ……

Thank you very much!

中国物理学会 Chinese Physical Society

中国科学院物理研究所 INSTITUTE OF PHYSICS CHINESE ACADEMY OF SCIENCES

JCR分区: **Q1**　中科院分区表：**一区Top期刊**

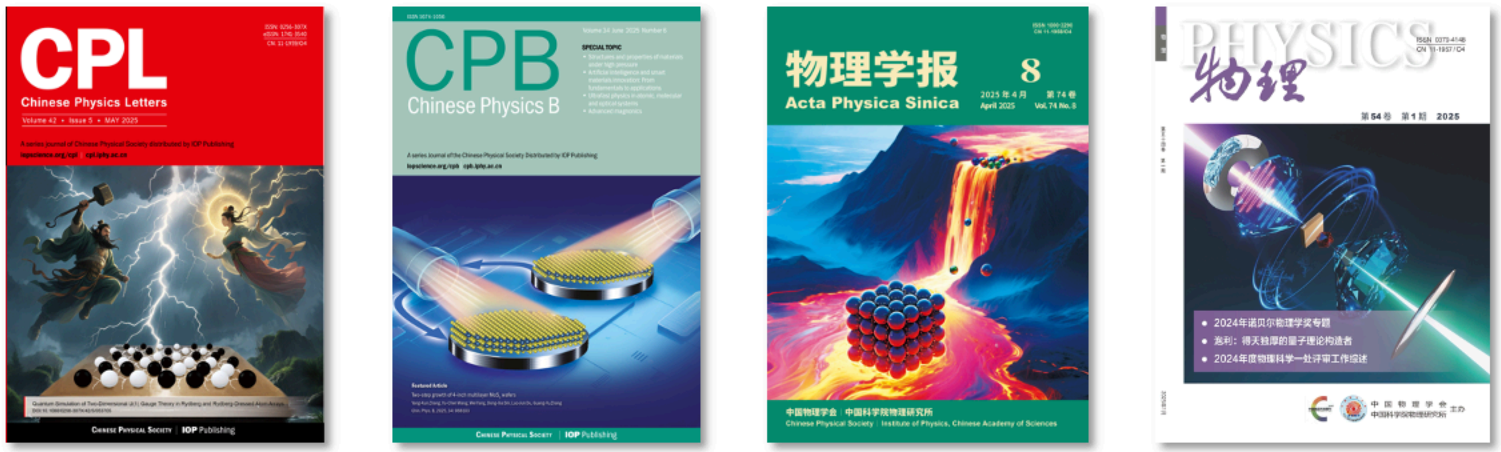

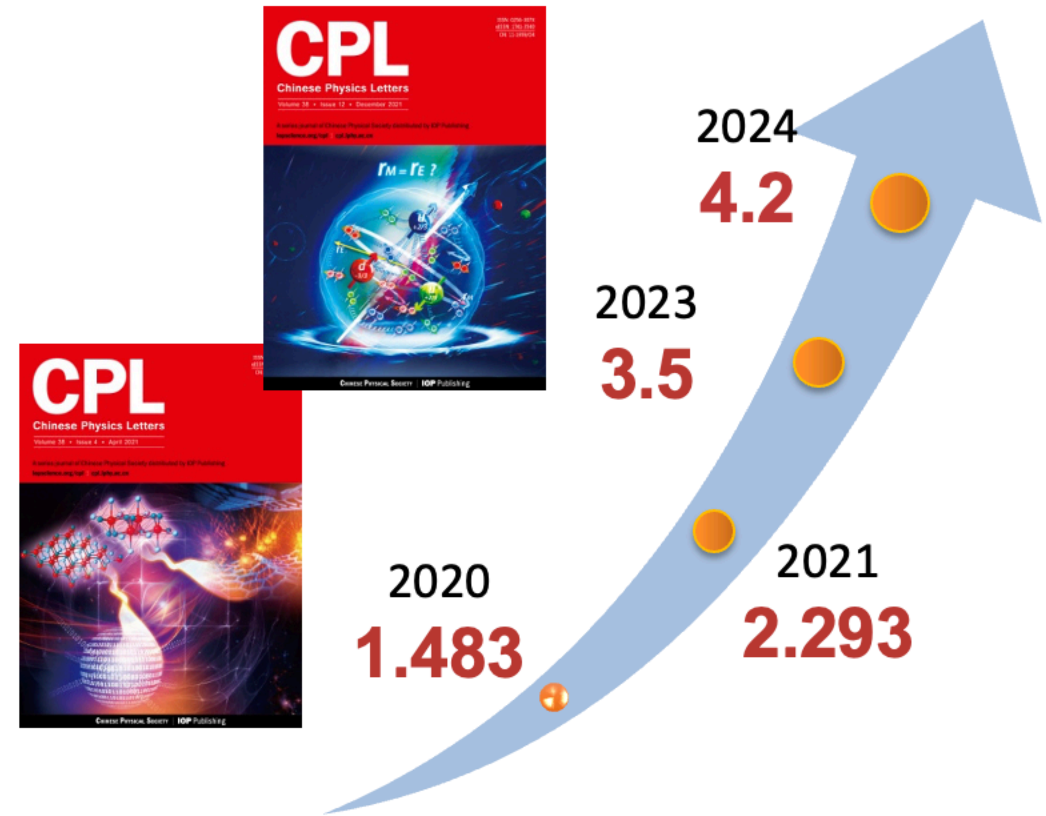

我国综合影响力最大的物理学期刊方阵

- 四刊由中国物理学会和中国科学院物理研究所主办
- 四刊年发文量2000多篇，占国内物理学期刊的70%
- 赵忠贤院士获得国家最高科学技术奖、国家自然科学奖一等奖和未来科学大奖的代表性成果之一，发表在CPL
- 薛其坤院士获得国家最高科学技术奖和未来科学大奖的代表性成果之一，发表在CPL

CPL EXPRESS LETTERS

Rapid Publish important and groundbreaking works

发文类型：中文/英文 | 学术/科普 | 研究论文/综述/观点/数据论文/仪器设备论文/程序代码论文

Thank you very much!